

The contour integral method for Feynman-Kac equation with two internal states

Fugui Ma^a, Lijing zhao^b, Yejuan Wang^a, Weihua Deng^{a,*}

^a*School of Mathematics and Statistics, Gansu Key Laboratory of Applied Mathematics and Complex Systems, Lanzhou University, Lanzhou 730000, Peoples Republic of China.*

^b*I. Research and Development Institute of Northwestern Polytechnical University in Shenzhen. II. School of Mathematics and Statistics, Northwestern Polytechnical University, Xian, 710129, Peoples Republic of China.*

Abstract

We develop the contour integral method for numerically solving the Feynman-Kac equation with two internal states [P. B. Xu and W. H. Deng, Math. Model. Nat. Phenom., 13 (2018), 10], describing the functional distribution of particle's internal states. The striking benefits are obtained, including spectral accuracy, low computational complexity, small memory requirement, etc. We perform the error estimates and stability analyses, which are confirmed by numerical experiments.

Keywords: Contour integral method, time marching scheme, Feynman-Kac equation, two internal states
2020 MSC: 65B15, 65E10, 65L30, 65R10, 65Z05, 68Q17

1. Introduction

The weak singularity at starting point of the solution and the non-locality of the time evolution operator of the Feynman-Kac equation [21] bring challenges on computational efficiency in numerically solving the equation. One of the most effective techniques to overcome the challenges is to analytically get the solution in frequency domain and then numerically do the inverse Laplace transform [22, 23, 20]. The contour integral method (CIM) is an efficient numerical method for solving the inverse Laplace transform [1, 20, 13].

Let us briefly introduce this method through the following toy model. Consider the time fractional initial value problem [11, 25]

$${}_0^C D_t^\alpha \mathbf{u}(t) + A\mathbf{u}(t) = \mathbf{b}(t), \quad \mathbf{u}(0) = \mathbf{u}_0, \quad (1)$$

where A is a matrix and ${}_0^C D_t^\alpha$ is the Caputo fractional derivative [11] with $t \in (0, T]$ and $0 < \alpha < 1$. Taking Laplace transform on (1), one can get the solution of the system in Laplace space, namely,

$$\widehat{\mathbf{u}}(z) = (z^\alpha I + A)^{-1} (z^{\alpha-1} \mathbf{u}_0 + \widehat{\mathbf{b}}(z)). \quad (2)$$

Further by performing the inverse Laplace transform on the solution in Laplace space, one get the solution of the system (1), i.e.,

$$\mathbf{u}(t) = \frac{1}{2\pi i} \int_{\sigma-i\infty}^{\sigma+i\infty} e^{zt} \widehat{\mathbf{u}}(z) dz, \quad \sigma > \sigma_0, \quad (3)$$

where σ_0 is called convergent abscissa. In practice, due to the complexity of $\widehat{\mathbf{u}}(z)$ and the high dimension of matrix A , it is hard to get the analytical solution of (1) by using the inverse Laplace transform (3). Hence, numerical methods are usually used to approximate (3). The CIM is one of the most efficient numerical methods to solve this indefinite integral.

The earliest discussion for CIM seems appeared in [1] by A. Talbot. Then, J. A. C. Weideman and other researchers gradually improved it and made it more efficient and widely applicable (see, e.g., [12, 7], etc). The basic idea of the

*Corresponding author

Email address: dengwh@lzu.edu.cn (Weihua Deng)

CIM method is to deform the integral line, since the original integration path of the inverse Laplace transform is a vertical line from negative infinity to positive infinity, which has many numerical challenges, e.g., the high frequency oscillation of the integrand. Fortunately, by deforming the vertical line into a curve, which starts and ends in the left half complex plane, the exponential decay of the integrand can be obtained by the exponential factor e^{zt} . Such a deformed line and the exponential decay of the integrand make it possible for an abnormal integral to be solved numerically, and Cauchy integral theorem can ensure that such a deformation can be carried out. More specifically, after deforming the integral line of (3) into a contour, which satisfies $Re(z) \rightarrow -\infty$ at each end, then, the exponential factor e^{zt} forces a rapid decay of the integrand as $Re(z) \rightarrow -\infty$, which greatly benefits to the convergence speed of numerical integral methods for solving the inverse Laplace transform.

Based on the aforementioned idea, we return to the original time fractional initial value problem (1). Suppose that there is an appropriate contour (for (1)) parameterized by

$$\Gamma : z = z(\phi), \quad -\infty < \phi < \infty. \quad (4)$$

Then the solution of (3) can be rewritten as

$$\mathbf{u}(t) = \frac{1}{2\pi i} \int_{-\infty}^{\infty} e^{z(\phi)t} \widehat{\mathbf{u}}(z(\phi)) z'(\phi) d\phi. \quad (5)$$

Approximating it by the trapezoidal rule with uniform step-length h , there is

$$\mathbf{u}(t) \approx \frac{h}{2\pi i} \sum_{k=-\infty}^{\infty} e^{z_k t} \widehat{\mathbf{u}}_k z'_k, \quad (6)$$

where $z_k = z(\phi_k)$, $z'_k = z'(\phi_k)$, $\widehat{\mathbf{u}}_k = \widehat{\mathbf{u}}(z_k)$ with $\phi_k = kh$. If the contour Γ is symmetric with respect to the real axis, A is a real matrix, then $\widehat{\mathbf{u}}(\bar{z}) = \overline{\widehat{\mathbf{u}}(z)}$, and after truncation, there is

$$\mathbf{u}(t) \approx \frac{h}{\pi} \text{Im} \left\{ \sum_{k=0}^{N-1} e^{z_k t} \widehat{\mathbf{u}}_k z'_k \right\}. \quad (7)$$

This is the CIM scheme of (1).

The key to design an efficient CIM scheme is to find the spectrum distribution of the matrix A , which determines how to choose an appropriate contour integral curve Γ .

The non-locality and the weakly singular kernel of the time fractional operator results to the $\mathcal{O}(N^2)$ computational cost for time-marching scheme and weak singularity of the solution. A lot of efforts have been made to efficiently deal with this difficulty (see, e.g., [6, 14] etc). Compared with the time-stepping methods (see eg. [14, 9]), the CIM scheme has the following cons and pros, when solving the nonlocal problems.

- Generally, the time-stepping methods need the memory of $\mathcal{O}(N)$ and have the computational complexity of $\mathcal{O}(N^2)$. While for the CIM scheme, the required memory is $\mathcal{O}(1)$ and the computational complexity is $\mathcal{O}(N)$.
- For the time-stepping methods, the solution at a given later time depends on the previous ones. While, for the CIM scheme, the solution can be directly computed at any desired time, without the information on earlier time.
- The computation cost of the CIM scheme mainly lies in solving the system (3), which can be parallelly computed with the rate of 100%.
- For the time-stepping methods, low regularity of the solution will make it hard to get a high convergence rate. This issue has little influence on the CIM scheme.
- (•) There is nothing perfect. Although, the CIM works well for the linear model, it is difficult to deal with the nonlinear one directly.

Above all, the CIM is a simple, time-saving, and efficient numerical method. To build a CIM scheme, the key is to choose an appropriate integral contour, which depends on the spectrum distribution of the matrix A . Currently, there are four types of popular integral contours used for the CIM, namely, Talbot's contour [1], parabolic contour e.g., [13], hyperbolic contour e.g., [19, 8], and other simple, closed, and positively oriented curves, e.g., [7, 5]. The CIM with these contours can be used to solve parabolic problems, e.g., [7, 12, 3], integral differential equation with convolution memory kernel [27, 2, 4], Black-Scholes and Heston equations [15], and other problems, e.g., [30, 31]. During these applications, the CIM behaves high numerical performance. This paper will develop the CIM scheme into the time fractional differential system, i.e., the Feynman-Kac equation with two internal states [21].

Feynman-Kac equation usually describes the distribution of a particular type of statistical observables, e.g., functional of the particle trajectory [24, 29, 21]. The model considered in this paper characterizes a specific functional: $A = \int_0^t U(j(\tau))d\tau$, where $j(\tau)$ represents the j -th internal state at time τ with values belonging to $\{1, 2, \dots, m\}$. The distribution of A in the frequency domain is governed by

$$\begin{cases} \mathbf{M}^T \frac{\partial}{\partial t} \mathbf{G} = (\mathbf{M}^T - \mathbf{I}) \text{diag}(B_{\alpha_1}^{-1}, B_{\alpha_2}^{-1}, \dots, B_{\alpha_m}^{-1}) \text{diag}(\mathfrak{D}_t^{1-\alpha_1}, \mathfrak{D}_t^{1-\alpha_2}, \dots, \mathfrak{D}_t^{1-\alpha_m}) \mathbf{G} \\ \quad - \rho \mathbf{M}^T \text{diag}(U(1), U(2), \dots, U(m)) \mathbf{G}, \quad t \in (0, T], \\ \mathbf{G}(\cdot, 0) = \mathbf{G}_0, \end{cases} \quad (8)$$

where M is the transition matrix of a Markov chain with dimension $m \times m$; $B_{\alpha_j}^{-1}$, $j = 1, 2, \dots, m$, are given positive real numbers; $\mathbf{G} = [G_1, G_2, \dots, G_m]^T$ denotes the solution of the model (8) with $G_j := G_j(\rho, t)$ represents the Laplace transform of $G_j(A, t)$ w.r.t. A ; and $G_j(A, t)$ is the probability density function (PDF) of finding the particle with the functional A in the j -th internal state at time t ; I is the identity matrix; 'diag' represents the diagonal matrix formed by its vector arguments; and $\mathfrak{D}_t^{1-\alpha_j}$, $j = 1, 2, \dots, m$, are the fractional substantial derivatives, defined as

$$\mathfrak{D}_t^{1-\alpha_j} G_j(\rho, t) := \left(\frac{\partial}{\partial t} + \rho U(j) \right) \frac{1}{\Gamma(\alpha_j)} \int_0^t \frac{\exp[-(t-\tau)\rho U(j)]}{(t-\tau)^{1-\alpha_j}} G_j(\rho, \tau) d\tau \quad (9)$$

with $0 < \alpha_j < 1$, $j = 1, 2, \dots, m$.

This paper is organized as follows. In Section 2, we give the regularity estimates on the solution of (8). In Section 3, the CIMs with parabolic contour and hyperbolic contour for the system (8) are built respectively. Also we perform the error estimate and stability analysis for these schemes. In addition, the parameters in parabolic and hyperbolic contours are optimally determined. To verify the efficiency of the CIMs, we also construct a time-marching scheme To provide a reference solution. Some numerical experiments are performed in Section 4 to show the high numerical performance of the CIMs in solving such a non-local system. Concluding remarks are presented in Section 5.

2. The continuous problem

In this section, we perform the regularity analysis for Problem (8).

2.1. Solution representations

We consider the Feynman-Kac equation with two internal states. Without loss of generality, the transition matrix M can be written as

$$M = \begin{bmatrix} p & 1-p \\ 1-b & b \end{bmatrix}, \quad (10)$$

where $p, b \in [0, 1]$, and $p + b \neq 1$. Then Problem (8) reduces to

$$\begin{cases} p \left(\frac{\partial}{\partial t} + U(1)\rho \right) G_1 + (1-b) \left(\frac{\partial}{\partial t} + U(2)\rho \right) G_2 = (p-1)B_{\alpha_1}^{-1} \mathfrak{D}_t^{1-\alpha_1} G_1 + (1-b)B_{\alpha_2}^{-1} \mathfrak{D}_t^{1-\alpha_2} G_2, \quad t \in (0, T], \\ (1-p) \left(\frac{\partial}{\partial t} + U(1)\rho \right) G_1 + b \left(\frac{\partial}{\partial t} + U(2)\rho \right) G_2 = (1-p)B_{\alpha_1}^{-1} \mathfrak{D}_t^{1-\alpha_1} G_1 + (b-1)B_{\alpha_2}^{-1} \mathfrak{D}_t^{1-\alpha_2} G_2, \quad t \in (0, T], \\ \mathbf{G}(\cdot, 0) = \mathbf{G}_0, \end{cases} \quad (11)$$

where $\mathbf{G}_0 = [G_{1,0}, G_{2,0}]^T$ is the initial value. After simple calculations, we can obtain from (11) that

$$\left(\frac{\partial}{\partial t} + U(1)\rho\right)G_1 + \left(\frac{\partial}{\partial t} + U(2)\rho\right)G_2 = 0.$$

Then, there is

$$\begin{cases} \left(\frac{\partial}{\partial t} + U(1)\rho\right)G_1 = \frac{1-p}{1-p-b}B_{\alpha_1}^{-1}\mathfrak{D}_t^{1-\alpha_1}G_1 + \frac{1-b}{p+b-1}B_{\alpha_2}^{-1}\mathfrak{D}_t^{1-\alpha_2}G_2, \\ \left(\frac{\partial}{\partial t} + U(2)\rho\right)G_2 = \frac{1-p}{p+b-1}B_{\alpha_1}^{-1}\mathfrak{D}_t^{1-\alpha_1}G_1 + \frac{1-b}{1-p-b}B_{\alpha_2}^{-1}\mathfrak{D}_t^{1-\alpha_2}G_2. \end{cases} \quad (12)$$

Denote $m_1 := \frac{1-p}{1-p-b}$, $m_2 := \frac{1-b}{1-p-b}$. For $0 < \alpha_1, \alpha_2 < 1$, if $G_j \in I_{0+}^{1-\alpha_j}[L_1(0, T)] := \{f : f(x) = {}_0I_t^{1-\alpha_j}\varphi(t), \varphi(t) \in L_1(0, T)\}$, then ${}_0D_t^{-\alpha_j}(e^{\rho U(j)t}G_j)|_{t=0} = 0$, $j = 1, 2$ (we note that the space $I_{0+}^{1-\alpha_j}[L_1(0, T)]$ only excludes some extreme functions such as $t^{-\beta}$, $\beta < \alpha_j$, so it is not a harsh requirement for G_j , see more details in [17]). By this, taking the Laplace transform on both sides of (12), we deduce

$$\begin{cases} \widehat{G}_1 = \left((z + \rho U(1)) - m_1 B_{\alpha_1}^{-1}(z + \rho U(1))^{1-\alpha_1}\right)^{-1} \left(-m_2 B_{\alpha_2}^{-1}(z + \rho U(2))^{1-\alpha_2} \widehat{G}_2 + G_{1,0}\right), \\ \widehat{G}_2 = \left((z + \rho U(2)) - m_2 B_{\alpha_2}^{-1}(z + \rho U(2))^{1-\alpha_2}\right)^{-1} \left(-m_1 B_{\alpha_1}^{-1}(z + \rho U(1))^{1-\alpha_1} \widehat{G}_1 + G_{2,0}\right). \end{cases} \quad (13)$$

Let

$$H(z) := \left\{[(z + \rho U(1))^{\alpha_1} - m_1 B_{\alpha_1}^{-1}][(z + \rho U(2))^{\alpha_2} - m_2 B_{\alpha_2}^{-1}] - m_1 m_2 B_{\alpha_1}^{-1} B_{\alpha_2}^{-1}\right\}^{-1}, \quad (14)$$

$$H_{\alpha_1}(z) := H(z) \left((z + \rho U(2))^{\alpha_2} - m_2 B_{\alpha_2}^{-1}\right), \quad (15)$$

and

$$H_{\alpha_2}(z) := H(z) \left((z + \rho U(1))^{\alpha_1} - m_1 B_{\alpha_1}^{-1}\right). \quad (16)$$

Then, the system (11) can be decoupled in Laplace space as

$$\begin{cases} \widehat{G}_1 = H_{\alpha_1}(z)(z + \rho U(1))^{\alpha_1-1}G_{1,0} - m_2 B_{\alpha_2}^{-1}H(z)(z + \rho U(1))^{\alpha_1-1}G_{2,0}, \\ \widehat{G}_2 = H_{\alpha_2}(z)(z + \rho U(2))^{\alpha_2-1}G_{2,0} - m_1 B_{\alpha_1}^{-1}H(z)(z + \rho U(2))^{\alpha_2-1}G_{1,0}. \end{cases} \quad (17)$$

2.2. Regularity

Define the sectors

$$\begin{aligned} \Sigma_\theta &:= \{z \in \mathbb{C} : |\arg(z)| \leq \theta, z \neq 0\}, \quad \theta \in (\pi/2, \pi); \\ \Sigma_{\theta,\delta} &:= \{z \in \mathbb{C} : |z| > \delta > 0, |\arg(z)| \leq \theta\}, \quad \theta \in (\pi/2, \pi). \end{aligned}$$

Take an integral contour

$$\Gamma_{\theta,\delta} := \{z \in \mathbb{C} : |z| = \delta > 0, |\arg(z)| \leq \theta\} \cup \{z \in \mathbb{C} : z = re^{\pm i\theta}, r \geq \delta > 0\},$$

oriented with an increasing imaginary part. Based on these analytic settings, we have the following estimates related to (11) or (17). See Appendix A for the proofs in details.

Lemma 2.1. *Let $z \in \Sigma_{\theta,\delta}$ and $\delta \geq 2 \max_{j=1,2} \{|\rho U(j)|\}$. For $0 < \alpha_j < 1$, there hold*

$$|(z + \rho U(j))^{-\alpha_j}| \leq 2|z|^{-\alpha_j}, \quad j = 1, 2.$$

Lemma 2.2. *Let $z \in \Sigma_{\theta,\delta}$ and $\delta \geq \max_{j=1,2} \{2|\rho U(j)|, 4^{1/\alpha_j}|m_j B_{\alpha_j}^{-1}|^{1/\alpha_j}\}$. For $0 < \alpha_j < 1$, there hold*

$$|((z + \rho U(j))^{\alpha_j} - m_j B_{\alpha_j}^{-1})^{-1}| \leq 4|z|^{-\alpha_j}, \quad j = 1, 2.$$

Lemma 2.3. Let $z \in \Sigma_{\theta, \delta}$, $\delta \geq \max \left\{ \max_{j=1,2} \left\{ 2|\rho U(j)|, 4^{1/\alpha_j} |m_j B_{\alpha_j}^{-1}|^{1/\alpha_j} \right\}, \left(32|m_1 m_2 B_{\alpha_1}^{-1} B_{\alpha_2}^{-1}| \right)^{1/(\alpha_1 + \alpha_2)} \right\}$. For $0 < \alpha_j < 1$, there hold

$$|H(z)| \leq 32|z|^{-\alpha_1 - \alpha_2}, \quad |H_{\alpha_j}(z)| \leq 8|z|^{-\alpha_j}, \quad j = 1, 2,$$

where $H(z)$ and $H_{\alpha_j}(z)$ are defined in (14), (15), and (16), respectively.

Lemma 2.4. Let $z \in \Sigma_{\theta, \delta}$ and δ satisfy the conditions in Lemma 2.3. For $0 < \alpha_j < 1$, there hold

$$|H_{\alpha_j}(z)(z + \rho U(j))^{\alpha_j - 1}| \leq 16|z|^{-1},$$

and

$$|H(z)(z + \rho U(j))^{\alpha_j - 1}| \leq 64|z|^{-1 - \alpha_j^*}, \quad j = 1, 2, \quad j \cdot j^* = 2.$$

Based on the above results, one can get the estimates on the solutions of (11).

Theorem 2.1. Under the conditions in Lemma 2.3, for given initial values $G_{j,0}$, $j = 1, 2$, and $t > 1/\delta$, the solutions of (11) satisfies

$$|G_j^{(q)}(t)| \leq \frac{32|m_{j^*} B_{\alpha_{j^*}}^{-1}|}{\pi} \left((-1/\cos(\theta)) t^{\alpha_{j^*} - q} e^{\cos(\theta)} + 2\theta \delta^{q - \alpha_{j^*}} e^{\delta T} \right) |G_{j^*,0}| + \frac{8}{\pi} \left((-1/\cos(\theta)) t^{-q} e^{\cos(\theta)} + 2\theta \delta^q e^{\delta T} \right) |G_{j,0}|,$$

for $q = 0, 1$, where $G_j^{(q)}(t)$ denote $\frac{\partial^q}{\partial t^q} G_j(t)$, $j = 1, 2$, and $j \cdot j^* = 2$.

Theorem 2.1 discovers the weak singularity of the solution bear to the origin, which usually weakens the performance of the time-marching schemes but, we will see in the following context, has no influence on the CIMs.

3. The schemes and error estimates for the Feynman-Kac system

In this section, for the system (11), the CIMs with two kinds of contours, i.e., parabolic contour and hyperbolic contour, are given. With careful analysis of the analytical domain of the solution in frequency domain, the parameters used in the contours are determined. The error estimates and stability analysis are presented. To give the reference solution for verifying the effectiveness of the CIMs, a time marching scheme is also designed.

3.1. The CIM schemes

Here we discuss two different integral contours [13] for the CIMs, which are parameterized by

$$(\text{Parabolic contour}) \quad \Gamma_1 : z(\phi) = \eta_1(i\phi + 1)^2, \quad -\infty < \phi < \infty, \quad (18)$$

and

$$(\text{Hyperbolic contour}) \quad \Gamma_2 : z(\phi) = \eta_2(1 + \sin(i\phi - \alpha)), \quad -\infty < \phi < \infty, \quad (19)$$

where $\eta_1, \eta_2 > 0$ and $\alpha > 0$ are the parameters to be determined. With these, the solutions $G_1(t)$, $G_2(t)$ can be represented as the infinite integrals with respect to ϕ , i.e.,

$$G_j(t) = I_j := \int_{-\infty}^{+\infty} v_j(t, \phi) d\phi, \quad j = 1, 2, \quad (20)$$

where

$$v_j(t, \phi) := \frac{1}{2\pi i} e^{z(\phi)t} \widehat{G}_j(z(\phi)) z'(\phi), \quad j = 1, 2 \quad (21)$$

with \widehat{G}_j defined in (13).

Applying the trapezoidal rule to compute the integral (20) with uniform steps h_m ($m = 1, 2$) for ϕ , one can numerically get the approximate solutions $G_{1,N}^{(m)}(t)$ and $G_{2,N}^{(m)}(t)$. Since the contours Γ_1 and Γ_2 are symmetric with respect to the real axis and $\widehat{G}_j(\overline{z(\phi)}) = \overline{\widehat{G}_j(z(\phi))}$, $j = 1, 2$, (20) can be approximated by

$$G_{j,N}^{(m)}(t) \approx I_{j,h_m,N} := h_m \sum_{k=1-N}^{N-1} v_j(t, \phi_k) = \frac{h_m}{\pi} \operatorname{Im} \left\{ \sum_{k=0}^{N-1} e^{z_k t} \widehat{G}_{j,k} z'_k \right\}, \quad j = 1, 2, \quad (22)$$

where $m = 1, 2$ denote the two different choices of the integral contours Γ_1 and Γ_2 .

It can be seen from (22) that the numerical solutions at current time are computed without knowing its information at previous times.

3.2. Quadrature error

The key issue to ensure the effectiveness and efficiency of the CIMs is to make all singular points of \widehat{G}_j locate at the left side of Γ_m and that the integrand of the indefinite integrals (20) has wide analytical open strips see, e.g., [13, 16].

3.2.1. Determination of the open strip

Since $z(\phi)$ in both of the integral contours (18) and (19) are analytical, the analytical properties of $v_j(t, \phi)$ in (21) is completely determined by $\widehat{G}_j(z(\phi))$. According to the expression of $\widehat{G}_j(z(\phi))$ in (17), the singularity mainly comes from $H(z)$.

Here we consider the case $U(j) \geq 0$, and denote $C_j := m_j B_{\alpha_j}^{-1}$, $j = 1, 2$. There are $C_j \neq 0$, $j = 1, 2$. The analytical domain of $H(z)$ are determined by the next proposition.

Proposition 3.1. *Let $z \in \sum_{\theta}$. If*

$$\operatorname{Re}((z + \rho U(j))^{\alpha_j}) > 2C_j, \quad j = 1, 2, \quad \text{or} \quad |\operatorname{Im}((z + \rho U(j))^{\alpha_j})| > |C_j|, \quad j = 1, 2, \quad (23)$$

then $H(z)$ is analytic.

See the proof in [Appendix B.1](#).

Remark 1. From (23), it can be further obtained that $H(z)$ is analytic if

$$\operatorname{Re}(z) > d_1 \quad \text{or} \quad |\operatorname{Im}(z)| > d_2, \quad (24)$$

where $d_1 := \max_{j=1,2} \left\{ (2|C_j| / \cos(\alpha_j \pi / 2))^{1/\alpha_j} - \operatorname{Re}(\rho U(j)) \right\}$ and $d_2 := \max_{j=1,2} \left\{ (|C_j| / \cos(\alpha_j \pi / 2))^{1/\alpha_j} - \operatorname{Im}(\rho U(j)) \right\}$. One can see [Appendix B.2](#) for more details.

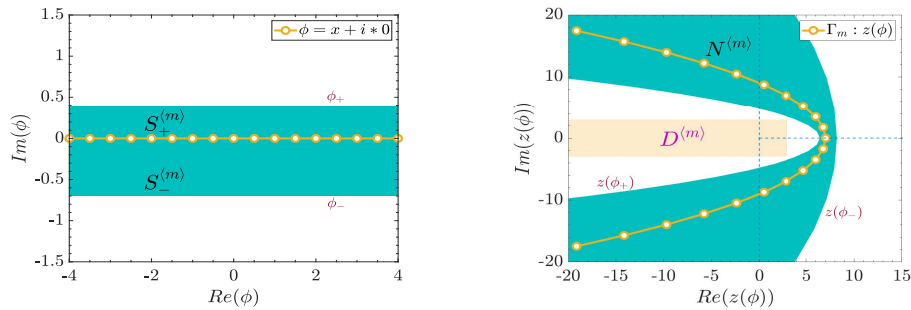


Figure 3.1: The schematic diagrams of open strip $S^{(m)}$ and the corresponding neighbourhood $N^{(m)}$; (left) is the horizontal open strip $S^{(m)}$; (right) is the neighborhood $N^{(m)}$ obtained by mapping the horizontal strip $S^{(m)}$ by the conformal transformation $z(\phi)$.

Given open strip

$$S^{(1)} := \{\phi = x + iy \in \mathbb{C} : -d < y < a < 1, x \in \mathbb{R} \text{ and } a, d > 0\}$$

or

$$S^{(2)} := \{\phi = x + iy \in \mathbb{C} : -\alpha < y < \pi/2 - \alpha - \delta, x \in \mathbb{R}, 0 < \alpha, \delta < \pi/2 \text{ and } \alpha < \pi/2 - \delta\},$$

then the integral contour Γ_1 or Γ_2 maps it into a neighbourhood, defined as $N^{(m)} := \{z(\phi) : \phi \in S^{(1)} \text{ or } S^{(2)}\}$. According to (24), there exists a domain $D^{(m)}$, such that $H(z)$ is analytical in the domain $\mathbb{C} \setminus D^{(m)}$, shown in Figure 3.1 (right). Hence, for any $z(\phi) \in N^{(m)} \subset \mathbb{C} \setminus D^{(m)}$, the integrand $v_j(t, \phi)$ is analytical. Since the integral contours Γ_1 and Γ_2 are holomorphic mappings, so, once $N^{(m)}$ are specified, the strips $S^{(1)}$ and $S^{(2)}$ can be accordingly determined.

For the consideration of convergence, we need to select the analytical domain $N^{(m)}$ as large as possible. Correspondingly, the optimum parameter a in $S^{(1)}$ is $a = 1 - \left[(d_1 + (d_1^2 + d_2^2)^{1/2})/(2\eta_1)\right]^{1/2}$ and the biggest value of d is given by (32); the optimal parameter δ in $S^{(2)}$ is $\delta = \arctan(d_2/(\eta_2 - d_1))$ and α is determined by maximizing $Q(\alpha) = \frac{\pi^2 - 2\pi\alpha - 2\pi\delta}{A(\alpha)}$ (see Subsection 3.2.3). For more details, one can see Appendix B.3.

3.2.2. Stability

Paved by the front part, the integrands $v_j(t, \phi)$ are analytical with respect to ϕ in the open strips $S^{(1)}$ and $S^{(2)}$. Now, for the CIMs (22) with the integral contours Γ_1 and Γ_2 , we have the following stability analyses.

Lemma 3.1 ([18], Lemma 1). *Take $L(x) := 1 + |\ln(1 - e^{-x})|$, $x > 0$, there hold*

$$\int_0^{+\infty} e^{-\gamma \cosh(x)} dx \leq L(\gamma), \quad \gamma > 0,$$

and

$$\int_\sigma^{+\infty} e^{-\gamma \cosh(x)} dx \leq (1 + L(\gamma))e^{-\gamma \cosh(\sigma)}, \quad \gamma > 0 \text{ and } \sigma > 0.$$

Lemma 3.2. *Let $v_1(t, \phi)$ be defined in (21) and $z(\phi)$ defined in (18) with $\phi = x + ir \in S^{(1)}$. For $t > 0$ and $B > 0$ defined in (B.10), we have*

$$|v_1(t, \phi)| \leq \frac{Be^{\eta_1 t}}{\pi} (|G_{1,0}| + \eta_1^{-\alpha_2} |G_{2,0}|) e^{-\eta_1 t x^2} \quad \forall \phi \in S^{(1)}. \quad (25)$$

Let $z(\phi)$ defined in (19) with $\phi = x + iy \in S^{(2)}$. For $t > 0$ and $0 < y < \min\{\alpha, \pi/2 - \alpha - \delta\}$, there holds

$$|v_1(t, \phi)| \leq \frac{8e^{\eta_2 t}}{\pi} \sqrt{\frac{1 + \sin(\alpha + y)}{1 - \sin(\alpha + y)}} \left(|G_{1,0}| + \frac{4|m_1 B_{\alpha_1}^{-1}|}{\eta_2^{\alpha_2} (1 - \sin(\alpha + y))^{\alpha_2}} |G_{2,0}| \right) e^{-\eta_2 t \sin \alpha \cosh x} \quad \forall \phi \in S^{(2)}. \quad (26)$$

For the integrand $v_2(t, \phi)$, similar estimates can be obtained.

The proof of Lemma 3.2 is given in Appendix B.4.

It can be seen from Lemma 3.2 that the decay of the solution mainly depends on the size of the real part. The stability results of the CIMs are given as follows.

Theorem 3.1. *Let $G_{1,N}^{(1)}(t)$ be defined in (22) with uniform steps h_1 . For $t > 0$ and $B > 0$ defined in (B.10), there holds*

$$|G_{1,N}^{(1)}(t)| \leq B \sqrt{\frac{\eta_1}{\pi}} (\eta_1^{-1} |G_{1,0}| + \eta_1^{-(1+\alpha_2)} |G_{2,0}|) t^{-1/2} e^{\eta_1 t}.$$

Let $G_{1,N}^{(2)}(t)$ be defined in (22) with uniform steps h_2 . For $t > 0$ and $0 < y < \min\{\alpha, \pi/2 - \alpha - \delta\}$, there holds

$$|G_{1,N}^{(2)}(t)| \leq \frac{16}{\pi} \sqrt{\frac{1 + \sin(\alpha + y)}{1 - \sin(\alpha + y)}} \left(|G_{1,0}| + \frac{4|m_1 B_{\alpha_1}^{-1}|}{\eta_2^{\alpha_2} (1 - \sin(\alpha + y))^{\alpha_2}} |G_{2,0}| \right) L(\eta_2 t \sin(\alpha)) e^{\eta_2 t}.$$

For $|G_{2,N}^{(m)}(t)|$, $m = 1, 2$, similar estimates can be obtained.

The proof of Theorem 3.1 can be found in Appendix B.5. Notice that $L(x)$ given in Lemma 3.1 is decreasing; $L(x) \rightarrow 1$ as $x \rightarrow \infty$ and $L(x) \sim |\ln x|$ as $x \rightarrow 0^+$. It can be seen that the CIMs are unconditionally stable with respect to the initial values.

3.2.3. Error estimates and determination of the optimal parameters

Here, we will determine the optimal parameters in the parabolic integral contour Γ_1 and hyperbolic contour Γ_2 , respectively, and prove that the CIMs (22) of the Feynmann-Kac equation with two internal states have spectral accuracy.

Denote $I_{j,h_m} := h_m \sum_{k=-\infty}^{\infty} v_j(t, kh_m)$. Then the error of the CIMs can be expressed as

$$E_{j,N}^{(m)} := |I_j - I_{j,h_m,N}| \leq DE^{(m)} + TE^{(m)}, \quad m, j = 1, 2,$$

where $TE^{(m)} = |I_{j,h_m} - I_{j,h_m,N}|$ is the truncation error and $DE^{(m)} := DE_+^{(m)} + DE_-^{(m)} := |I_j - I_{j,h_m}|$ is the discretization error. The standard estimates of the discretization error are shown in the following lemma.

Lemma 3.3 ([13] Theorem 2.1). *Consider the absolutely convergent integral*

$$I := \int_{-\infty}^{\infty} g(u) du,$$

and its infinite and trapezoidal approximation

$$I_\tau := \tau \sum_{k=-\infty}^{\infty} g(k\tau).$$

Let $w = u + iv$, with u and v real. Suppose $g(w)$ is analytic in the strip $-d < v < c$, for some $c > 0$, $d > 0$, with $g(w) \rightarrow 0$ uniformly as $|w| \rightarrow \infty$ in this strip. Suppose further that for some $M_+ > 0$, $M_- > 0$, the function $g(w)$ satisfies

$$\int_{-\infty}^{\infty} |g(u + ir)| du \leq M_+, \quad \int_{-\infty}^{\infty} |g(u - is)| du \leq M_-, \quad (27)$$

for all $0 < r < c$, $0 < s < d$. Then the discretization error

$$DE := |I - I_\tau| \leq DE_+ + DE_-,$$

where

$$DE_+ = \frac{M_+}{e^{2\pi c/\tau} - 1}, \quad DE_- = \frac{M_-}{e^{2\pi d/\tau} - 1}.$$

Based on lemma 3.3, for the CIMs with the integral contour Γ_1 and Γ_2 , we have the following error estimates.

Theorem 3.2. *Let $G_1(t)$ and $G_{1,N}^{(1)}(t)$ be the solutions of (11) and (22) with uniform step-size h_1 . Given $a > 0$, for $t > 0$, $h_1 = \mathcal{O}(1/N)$, there holds*

$$|G_1(t) - G_{1,N}^{(1)}(t)| \leq B \sqrt{\frac{\eta_1}{\pi}} t^{-1/2} \left(\eta_1^{-1} |G_{1,0}| + \eta_1^{-(1+\alpha_2)} |G_{2,0}| \right) \left(\frac{e^{\eta_1 t}}{e^{2\pi a/h_1} - 1} + \frac{e^{\pi^2/(\eta_1 t h_1^2)}}{e^{2\pi^2/(\eta_1 t h_1^2) - 2\pi/h_1} - 1} + \frac{e^{\eta_1 t}}{e^{\eta_1 t (N h_1)^2}} \right).$$

Let $G_{1,N}^{(2)}(t)$ be the solution of (22) with uniform step-size h_2 . For $t > 0$, $h_2 = \mathcal{O}(1/N)$, and $0 < y < \min\{\alpha, \pi/2 - \alpha - \delta\}$, we have

$$\begin{aligned} |G_1(t) - G_{1,N}^{(2)}(t)| &\leq \frac{16}{\pi} \sqrt{\frac{1 + \sin(\alpha + y)}{1 - \sin(\alpha + y)}} \left(|G_{1,0}| + \frac{4 |m_1 B_{\alpha_1}^{-1}|}{\eta_2^{\alpha_2} (1 - \sin(\alpha + y))^{\alpha_2}} |G_{2,0}| \right) e^{\eta_2 t} \\ &\quad \times \left(\frac{L(\eta_2 t \sin(\alpha))}{e^{2\pi(\pi/2 - \alpha - \delta)/h_2} - 1} + \frac{L(\eta_2 t \sin(\alpha))}{e^{2\pi\alpha/h_2} - 1} + \frac{1 + L(\eta_2 t \sin(\alpha))}{e^{\eta_2 t \sin \alpha \cosh(N h_2)}} \right). \end{aligned}$$

For $|G_2(t) - G_{2,N}^{(m)}(t)|$, $m = 1, 2$, there are similar estimates hold.

PROOF. Let $v_j(t, \phi)$, $j = 1, 2$ be defined as in (21) with $z(\phi)$ defined as (18) and (19), respectively.

To proof the first part of the theorem, we need to perform error estimates about $DE_+^{(1)}$, $DE_-^{(1)}$, and $TE^{(1)}$.

Estimate of $DE_+^{(1)}$: By (25) in Lemma 3.2, for $t > 0$, $0 < a < 1$, there is

$$\begin{aligned} \int_{-\infty}^{\infty} |v_1(t, x + ia)| dx &\leq \frac{\eta_1 e^{\eta_1 t}}{\pi} \left(\frac{16}{\eta_1(1-a)} |G_{1,0}| + \frac{64 |m_1 B_{\alpha_1}^{-1}|}{\eta_1^{1+\alpha_2}(1-a)^{1+2\alpha_2}} |G_{2,0}| \right) \int_{-\infty}^{\infty} e^{-\eta_1 t x^2} dx \\ &\leq B \sqrt{\frac{\eta_1}{\pi}} t^{-1/2} e^{\eta_1 t} \left(\eta_1^{-1} |G_{1,0}| + \eta_1^{-(1+\alpha_2)} |G_{2,0}| \right) < \infty, \end{aligned}$$

where B is defined in (B.10). Then, according to Lemma 3.2, we have

$$DE_+^{(1)} \leq B \sqrt{\frac{\eta_1}{\pi}} t^{-1/2} e^{\eta_1 t} \left(\eta_1^{-1} |G_{1,0}| + \eta_1^{-(1+\alpha_2)} |G_{2,0}| \right) \frac{1}{e^{2\pi a/h_1} - 1}. \quad (28)$$

Thus,

$$DE_+^{(1)} = \mathcal{O}\left(e^{\eta_1 t - 2\pi a/h_1}\right), \quad h_1 \rightarrow 0. \quad (29)$$

Estimate of $DE_-^{(1)}$: Similarly, for $t > 0$, there holds

$$\begin{aligned} \int_{-\infty}^{\infty} |v_1(t, x - id)| dx &\leq \frac{\eta_1 e^{\eta_1(1+d)^2 t}}{\pi} \left(16\eta_1^{-1} |G_{1,0}| + 64 |m_1 B_{\alpha_1}^{-1}| \eta_1^{-(1+\alpha_2)} |G_{2,0}| \right) \int_{-\infty}^{\infty} e^{-\eta_1 t x^2} dx \\ &\leq B \sqrt{\frac{\eta_1}{\pi}} t^{-1/2} e^{\eta_1(1+d)^2 t} \left(\eta_1^{-1} |G_{1,0}| + \eta_1^{-(1+\alpha_2)} |G_{2,0}| \right) < \infty. \end{aligned}$$

By Lemma 3.2, we have

$$DE_-^{(1)} \leq B \sqrt{\frac{\eta_1}{\pi}} t^{-1/2} e^{\eta_1(1+d)^2 t} \left(\eta_1^{-1} |G_{1,0}| + \eta_1^{-(1+\alpha_2)} |G_{2,0}| \right) \frac{1}{e^{2\pi d/h_1} - 1}, \quad (30)$$

and

$$DE_-^{(1)} = \mathcal{O}\left(e^{\eta_1(1+d)^2 t - 2\pi d/h_1}\right), \quad h_1 \rightarrow 0. \quad (31)$$

Denote $\omega(d) = \eta_1(1+d)^2 t - 2\pi d/h_1$. Then the ‘best’ choice of d is obtained by setting $\omega'(d) = 0$ (see [13]), which yields

$$d = \frac{\pi}{\eta_1 t h_1} - 1. \quad (32)$$

Now, we have

$$DE_-^{(1)} \leq B \sqrt{\frac{\eta_1}{\pi}} t^{-1/2} \left(\eta_1^{-1} |G_{1,0}| + \eta_1^{-(1+\alpha_2)} |G_{2,0}| \right) \frac{e^{\pi^2/(\eta_1 t h_1^2)}}{e^{2\pi^2/(\eta_1 t h_1^2) - 2\pi/h_1} - 1}$$

and

$$DE_-^{(1)} = \mathcal{O}\left(e^{-\pi^2/(\eta_1 t h_1^2) + 2\pi/h_1}\right), \quad h_1 \rightarrow 0.$$

Estimate of $TE^{(1)}$: By the definition of I_{1,h_1} and $I_{1,h_1,N}$, we deduce

$$|I_{1,h_1} - I_{1,h_1,N}| \leq h_1 \sum_{k=N}^{\infty} (|v_1(t, kh_1)| + |v_1(t, -kh_1)|) \leq 2h_1 \sum_{k=N}^{\infty} |v_1(t, kh_1)|.$$

According to (25) in Lemma 3.2, we have

$$\begin{aligned} h_1 \sum_{k=N}^{\infty} |v_1(t, kh_1)| &\leq \frac{\eta_1 B e^{\eta_1 t}}{\pi} \left(\eta_1^{-1} |G_{1,0}| + \eta_1^{-(1+\alpha_2)} |G_{2,0}| \right) \int_{Nh_1}^{\infty} e^{-x^2 \eta_1 t} dx \\ &\leq B \sqrt{\frac{\eta_1}{\pi}} t^{-1/2} \left(\eta_1^{-1} |G_{1,0}| + \eta_1^{-(1+\alpha_2)} |G_{2,0}| \right) e^{\eta_1 t(1-(Nh_1)^2)}. \end{aligned} \quad (33)$$

Thus,

$$TE^{(1)} \leq B \sqrt{\frac{\eta_1}{\pi}} t^{-1/2} \left(\eta_1^{-1} |G_{1,0}| + \eta_1^{-(1+\alpha_2)} |G_{2,0}| \right) e^{\eta_1 t (1 - (Nh_1)^2)} \quad (34)$$

and

$$TE^{(1)} = \mathcal{O} \left(e^{\eta_1 t (1 - (Nh_1)^2)} \right), \quad N \rightarrow +\infty. \quad (35)$$

Combining (28), (30), and (34) results in the first part of the theorem.

As for the hyperbolic integral contour with the strip $S^{(2)}$, similar to the previous analyses, we will directly give the corresponding results in the sequence.

Estimate of $DE_+^{(2)}$: By (26) in Lemma 3.2 and Lemma 3.3, for $t > 0$ and $0 < y < \pi/2 - \alpha - \delta$, there holds

$$DE_+^{(2)} \leq \frac{16}{\pi} \sqrt{\frac{1 + \sin(\alpha + y)}{1 - \sin(\alpha + y)}} \left(|G_{1,0}| + \frac{4 |m_1 B_{\alpha_1}^{-1}|}{\eta_2^{\alpha_2} (1 - \sin(\alpha + y))^{\alpha_2}} |G_{2,0}| \right) \frac{e^{\eta_2 t L(\eta_2 t \sin(\alpha))}}{e^{2\pi(\pi/2 - \alpha - \delta)/h_2} - 1}, \quad (36)$$

and

$$DE_+^{(2)} = \mathcal{O} \left(e^{\eta_2 t - 2\pi(\pi/2 - \alpha - \delta)/h_2} \right), \quad h_2 \rightarrow 0. \quad (37)$$

Estimate of $DE_-^{(2)}$: Similarly, there are

$$DE_-^{(2)} \leq \frac{16}{\pi} \sqrt{\frac{1 + \sin(\alpha + y)}{1 - \sin(\alpha + y)}} \left(|G_{1,0}| + \frac{4 |m_1 B_{\alpha_1}^{-1}|}{\eta_2^{\alpha_2} (1 - \sin(\alpha + y))^{\alpha_2}} |G_{2,0}| \right) \frac{e^{\eta_2 t L(\eta_2 t \sin(\alpha))}}{e^{2\pi\alpha/h_2} - 1}, \quad (38)$$

and

$$DE_-^{(2)} = \mathcal{O} \left(e^{\eta_2 t - 2\pi\alpha/h_2} \right), \quad h_2 \rightarrow 0. \quad (39)$$

Estimate of $TE^{(2)}$: From (26) and Lemma 3.1, there holds

$$\begin{aligned} h_2 \sum_N |v_1(t, kh_2)| &\leq \frac{8}{\pi} \sqrt{\frac{1 + \sin(\alpha + y)}{1 - \sin(\alpha + y)}} \left(|G_{1,0}| + \frac{4 |m_1 B_{\alpha_1}^{-1}|}{\eta_2^{\alpha_2} (1 - \sin(\alpha + y))^{\alpha_2}} |G_{2,0}| \right) \int_{Nh_2}^{+\infty} e^{\eta_2 t - \eta_2 t \sin \alpha \cosh x} dx \\ &\leq \frac{8}{\pi} (1 + L(\eta_2 t \sin \alpha)) \sqrt{\frac{1 + \sin(\alpha + y)}{1 - \sin(\alpha + y)}} \left(|G_{1,0}| + \frac{4 |m_1 B_{\alpha_1}^{-1}|}{\eta_2^{\alpha_2} (1 - \sin(\alpha + y))^{\alpha_2}} |G_{2,0}| \right) e^{\eta_2 t - \eta_2 t \sin(\alpha) \cosh(Nh_2)}. \end{aligned}$$

Thus

$$TE^{(2)} \leq \frac{16}{\pi} (1 + L(\eta_2 t \sin \alpha)) \sqrt{\frac{1 + \sin(\alpha + y)}{1 - \sin(\alpha + y)}} \left(|G_{1,0}| + \frac{4 |m_1 B_{\alpha_1}^{-1}|}{\eta_2^{\alpha_2} (1 - \sin(\alpha + y))^{\alpha_2}} |G_{2,0}| \right) e^{\eta_2 t - \eta_2 t \sin(\alpha) \cosh(Nh_2)}, \quad (40)$$

and

$$TE^{(2)} = \mathcal{O} \left(e^{\eta_2 t (1 - \sin \alpha \cosh(h_2 N))} \right), \quad N \rightarrow +\infty. \quad (41)$$

Together with (36), (38) and (40), we finish the second part of the theorem.

Similar estimates on $|G_2(t) - G_{2,N}^{(m)}(t)|$ can be obtained.

Next, we determine the optimal parameters in the integral contours Γ_1 and Γ_2 . Reference [13] has provided a technical method to determine these parameters under ideal conditions, i.e., asymptotically balancing $DE_+^{(m)}$, $DE_-^{(m)}$, and $TE^{(m)}$, $m = 1, 2$. Based on this idea, we will optimize these parameters in our situations.

For Γ_1 , by asymptotically balancing $DE_+^{(1)}$, $DE_-^{(1)}$, and $TE^{(1)}$, it needs

$$\eta_1 t - \frac{2\pi a}{h_1} = \frac{-\pi^2}{\eta_1 t h_1^2} + \frac{2\pi}{h_1} = \eta_1 t (1 - (Nh_1)^2). \quad (42)$$

Then we obtain the optimal parameters used in the contour Γ_1 , i.e.,

$$\eta_1^* = \frac{\pi \sqrt{2aq^3} N}{2a} \frac{1}{t}, \quad \text{and} \quad h_1^* = \frac{\sqrt{2aq}}{q} \frac{1}{N}, \quad (43)$$

where $q := 1 + a - \sqrt{a^2 + 2a}$ with $1/4 < a < 1$. With these optimal parameters, the corresponding convergence order of the CIM with the parabolic contour Γ_1 are

$$E_{j,N}^{(1)} = \mathcal{O}\left(e^{-\left(\pi\sqrt{2aq} - \pi\sqrt{2aq^3/(2a)}\right)N}\right), \quad j = 1, 2.$$

Furthermore, as mentioned in [13], the parameter η_1^* in (43) depends on time t , which means that the integral contour changes with time t . The ideal situation is that we find a fixed integral contour that satisfies the condition (24) which does not change over time t . Reviewing the error estimates $DE_+^{(1)}$, $DE_-^{(1)}$, and $TE^{(1)}$, it can be found that $DE_+^{(1)}$ and $DE_-^{(1)}$ increase with t , and TE decreases with t . If we want a small absolute error on the interval $t_0 \leq t \leq t_1 = T$, $t_0 > 0$, we can modify (42) as

$$\eta_1 t_1 - \frac{2\pi a}{h_1} = \frac{-\pi^2}{\eta_1 t_1 h_1^2} + \frac{2\pi}{h_1} = \eta_1 t_0 (1 - (Nh_1)^2). \quad (44)$$

Denote $\Lambda = t_1/t_0$, which increases from 1. After solving (44), we have

$$\eta_1 = \frac{\pi q \sqrt{q^2(1-\Lambda) + 2a\Lambda q}}{q(1-\Lambda) + 2a\Lambda} \frac{N}{t_1}, \quad h_1 = \frac{\sqrt{q^2(1-\Lambda) + 2a\Lambda q}}{q} \frac{1}{N}, \quad (45)$$

and the corresponding convergence order of the CIMs are

$$E_{j,N}^{(1)} = \mathcal{O}\left(e^{-P(\Lambda)N}\right), \quad j = 1, 2, \quad N \rightarrow +\infty, \quad (46)$$

where $P(\Lambda) = \frac{\pi(q-2a)\sqrt{q^2(1-\Lambda)+2a\Lambda q}}{q(\Lambda-1)+2a\Lambda}$.

For Γ_2 , similar to the previous analyses of Γ_1 , when $t \in [t_0, t_0\Lambda]$, $t_0 > 0$, $T = t_1 = t_0\Lambda$, the discretization error $DE_-^{(2)}$ increases with t and the truncation error $TE^{(2)}$ decreases with t . Thus, $DE_-^{(2)}$ and $TE^{(2)}$ can be modified as

$$DE_-^{(2)*} = \mathcal{O}\left(e^{\eta_2 t_1 - 2\pi\alpha/h_2}\right), \quad TE^{(2)*} = \mathcal{O}\left(e^{\eta_2 t_0 (1 - \sin\alpha \cosh(h_2 N))}\right).$$

By asymptotically balancing $DE_+^{(2)}$, $DE_-^{(2)*}$ and $TE^{(2)*}$, there holds

$$\frac{-2\pi(\pi/2 - \alpha - \delta)}{h_2} = \eta_2 t_1 - \frac{2\pi\alpha}{h_2} = \eta_2 t_0 (1 - \sin\alpha \cosh(h_2 N)).$$

Solving it results in

$$h_2 = \frac{A(\alpha)}{N}, \quad \eta_2 = \frac{4\pi\alpha - \pi^2 + 2\pi\delta}{A(\alpha)} \frac{N}{t_1}, \quad \text{and } A(\alpha) = \cosh^{-1}\left(\frac{(\pi - 2\alpha - 2\delta)\Lambda + (4\alpha - \pi + 2\delta)}{(4\alpha - \pi + 2\delta)\sin(\alpha)}\right), \quad (47)$$

with and

$$E_{j,N}^{(2)} = \mathcal{O}\left(e^{-Q(\alpha)N}\right), \quad j = 1, 2, \quad N \rightarrow +\infty,$$

where $Q(\alpha) = \frac{\pi^2 - 2\pi\alpha - 2\pi\delta}{A(\alpha)}$. For fixed Λ and δ , the optimal parameter α can be obtained by maximizing $Q(\alpha)$, which is similar to the results of [13].

To sum up: The specific strategy we determine the integral contours Γ_1 is as follows

- a) given a with $1/4 < a < 1$; compute $q = 1 + a - \sqrt{a^2 + 2a}$;
- b) determine η_1 and h_1 by (45);
- c) let $\phi = x + iy$ with $y = 0$ and $x \in \mathbb{R}$;
- d) determine Γ_1 as defined in (18).

The specific strategy we determine the integral contours Γ_2 is as below

- given an interval $[t_0, t_1]$; compute $\Lambda = t_1/t_0$;
- given δ with $0 < \delta < \pi/2$; determine the optimal parameter α^* by maximizing $Q(\alpha) = \frac{\pi^2 - 2\pi\alpha - 2\pi\delta}{A(\alpha)}$;
- compute $A(\alpha^*)$ and then h_2 and η_2 in (47);
- let $\phi = x + iy$ with $x \in \mathbb{R}$ and a given y , $0 < y < \min\{\alpha, \pi/2 - \alpha - \delta\}$;
- determine Γ_2 as defined in (19).

Through the above analyses, it can be found that the CIMs constructed in this paper with given optimal step-sizes and parameters have the convergence order of $\mathcal{O}(e^{-cN})$. That is, the CIMs in our paper have spectral accuracy.

3.3. The time-matching schemes

In this subsection, in order to verify the high numerical performance of the CIMs (22) with the determined integral contours Γ_1 and Γ_2 , we also show another numerical methods to solve (11), i.e., the time-marching schemes (TMs) e.g. [10], etc.

Let h be the discrete stepsize and $t_n = nh$, $n = 0, 1, 2, \dots, M$, $M = \frac{T}{h}$. Integrating both sides of (12) from 0 to t and letting $t = t_{n+1}$, we get the integral form (C.1) and (C.2).

The specific TMs are shown in Appendix C, in which the following two formulas are used.

$$\begin{aligned} \int_0^t \mathfrak{D}_s^{1-\alpha_j} G_j(., \rho) ds &= \frac{1}{\Gamma(\alpha_j)} \int_0^t \frac{\partial}{\partial s} \int_0^s \frac{e^{-(s-\tau)\rho U(j)}}{(s-\tau)^{1-\alpha_j}} G_j(\rho, \tau) d\tau ds + \frac{\rho U(j)}{\Gamma(\alpha_j)} \int_0^t \int_0^s \frac{e^{-(s-\tau)\rho U(j)}}{(s-\tau)^{1-\alpha_j}} G_j(\rho, \tau) d\tau ds \\ &= \frac{1}{\Gamma(\alpha_j)} \left(\int_0^t \frac{e^{-(t-\tau)\rho U(j)}}{(t-\tau)^{1-\alpha_j}} G_j(\rho, \tau) d\tau + (\rho U(j))^{1-\alpha_j} \gamma(\alpha_j, 1) \int_0^t G_j(\rho, \tau) d\tau \right), \quad j = 1, 2, \end{aligned} \quad (48)$$

where $\gamma(\alpha_j, 1)$ are the incomplete gamma function with different parameters α_j , $j = 1, 2$. For the first term of the right hand of 48, we perform the linear interpolation on the integrand, that is

$$\begin{aligned} \int_{t_n}^{t_{n+1}} e^{-\rho U(j)(t_{n+1}-\tau)} (t_{n+1}-\tau)^{\alpha_j-1} G_j(\rho, \tau) d\tau &\approx \int_{t_n}^{t_{n+1}} (t_{n+1}-\tau)^{\alpha_j-1} \frac{G_j(., t_{n+1})(\tau - t_n) + e^{-\rho U(j)h} G_j(., t_n)(t_{n+1} - \tau)}{h} d\tau \\ &= \frac{h^{\alpha_j}}{\alpha_j(\alpha_j + 1)} \left(\alpha_j e^{-\rho U(j)h} G_j(., t_n) + G_j(., t_{n+1}) \right), \quad j = 1, 2. \end{aligned}$$

Based on these results, after doing some calculations, the time-marching schemes of (11) are designed as in (C.5), (C.7).

4. Numerical Results

In this section, we use two examples to evaluate the effectiveness of the CIM. We choose $p = 2/3$, $b = 3/4$, $B_{\alpha_1}^{-1} = B_{\alpha_2}^{-1} = 1$, and the optimal parameters are given in (45) and (47). Take $a = 0.9875$ and $\delta = 0.1123$ such that the contours Γ_1 and Γ_2 satisfy the condition (24). Here, we remark that the computing environment for all examples is *Intel(R) Core(TM) i7-7700 CPU @3.60GHz, MATLAB R2018a*.

4.1. Example 1

This example is used to verify that the CIMs (22) have spectral accuracy. We choose the absolute error as a function of N , i.e.,

$$error(N) = \max_{t_0 \leq t \leq \Lambda t_0} \left| G_j(., t) - G_{j,N}^{(m)}(., t) \right|, \quad m, j = 1, 2, \quad (49)$$

where $G_j(., t)$ is the reference solution computed by the time-marching schemes with much small stepsize, and $G_{j,N}^{(m)}(., t)$ is the numerical solution obtained by the CIM with parabolic contour Γ_1 and hyperbolic contour Γ_2 , respectively. Then, the absolute errors of the CIMs at different given times and the numerical solutions of the system are shown in Figure 4.1 and Figure 4.2.

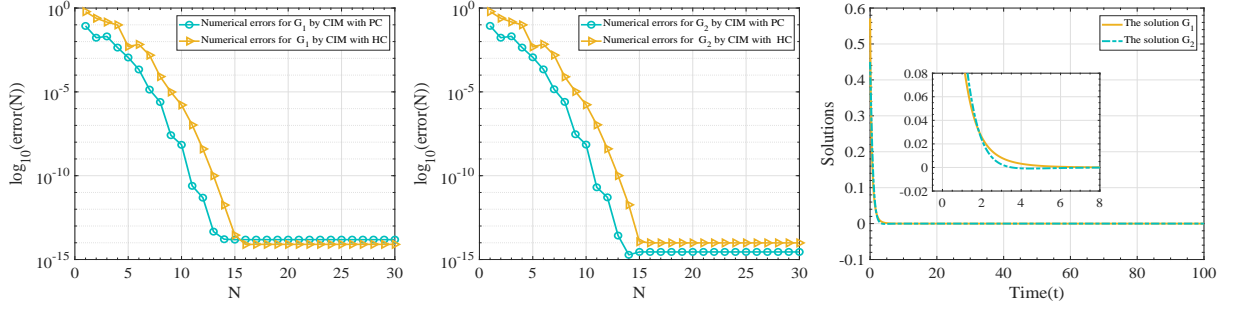


Figure 4.1: The absolute errors at time $t = 100$ and the numerical solutions of the system (11); (left) and (center) are the absolute errors for the CIM with Γ_1 and Γ_2 , respectively; The parameters are set as $N = 30$, $\Lambda=5$, $\alpha_1 = 0.6$, $\alpha_2 = 0.4$, $U(1) = 1$, $U(2) = 1$, $\rho = 1.5$, and the initial values $G_{1,0} = 0.55$, $G_{2,0} = 0.45$; (right) are the numerical solutions obtained by using TMs with the same parameters and the number of discrete points $M = 2^{15}$ and $T = 100$.

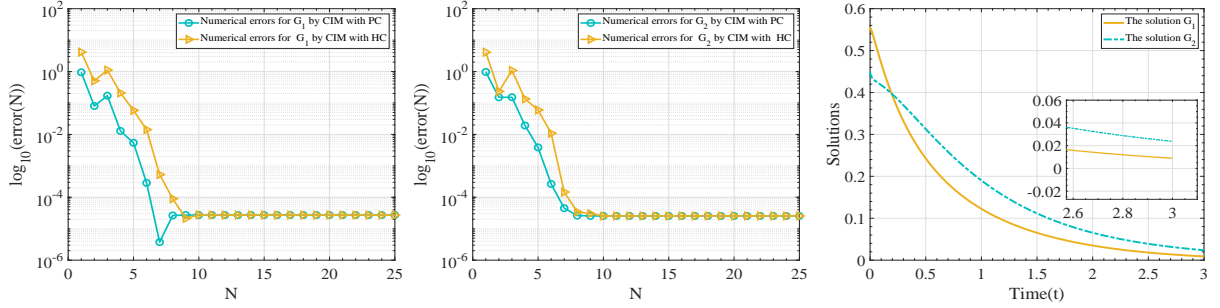


Figure 4.2: The absolute errors at time $t = 3$ and the numerical solutions of the system (11); (left) and (center) are the absolute errors of the CIM with Γ_1 and Γ_2 , respectively; The parameters are set as $N = 25$, $\Lambda=5$, $\alpha_1 = 0.82$, $\alpha_2 = 0.59$, $U(1) = 0.89$, $U(2) = 0.68$, $\rho = 1.5$, and the initial values $G_{1,0} = 0.55$ and $G_{2,0} = 0.45$; (right) are the numerical solutions obtained by using TMs with the same parameters and the number of discrete points $M = 2^{12}$ and $T = 3$.

Table 1: The CPU time cost of CIM and TMS for the system (11) at time $t = 3$.

Accuracy	PDF	CIM-PC		CIM-HC		TMs	
		N	time(s)	N	time(s)	M	time (s)
10^{-2}	$G_1(., t)$	5	4.1903e-03	3	1.0031e-02	10	2.0175e-03
	$G_2(., t)$	5	3.4310e-03	3	1.2785e-02	24	5.2115e-03
10^{-3}	$G_1(., t)$	9	1.2757e-03	7	1.6547e-03	10	2.2867e-03
	$G_2(., t)$	9	1.1832e-03	7	2.0558e-03	283	1.6356e-01
10^{-4}	$G_1(., t)$	13	3.0482e-03	8	1.2326e-03	630	6.7298e-01
	$G_2(., t)$	14	2.3619e-03	8	1.4250e-03	1953	5.9451e+00

Given a specific accuracy to be reached, the number of discrete points and the time cost of the CIMs and TMs are shown in Table 1, in which the parameters used are consistent with those in Figure 3, and we treat the numerical solutions obtained by TMs with $M = 2^{12}$.

One can see from Figures 4.1-4.3 as well as Table 1 that the CIMs with parabolic contour and hyperbolic contour are much effective and time-saving in solving the Feynman-Kac equation with two internal states. Also they have spectral accuracy.

4.2. Example 2

As a physical application, we calculate the average occupation time of each internal state by using the CIMs. As the matter of fact, the average occupation time of the first internal state can be calculated as the solution of the system

(8) by taking

$$U[j(\tau)] = \begin{cases} 1, & j(\tau) = 1, \\ 0, & \text{else,} \end{cases} \quad (50)$$

in the functional $A = \int_0^\tau [U(j(\tau))]d\tau$. While taking $U(1) = 0$ and $U(2) = 1$, it works for the second internal state. Take $\alpha_1 = \alpha_2$. According to the theoretical results presented in [21], the average occupation time of the first state is

$$\langle A \rangle \sim \frac{\varepsilon_1}{\varepsilon_1 + \varepsilon_2} t, \quad \text{for large } t, \quad (51)$$

where ε_1 and ε_2 are the initial distributions (replacing the coefficient by $\varepsilon_2/(\varepsilon_1 + \varepsilon_2)$ for the second internal state). In this paper, $\langle A \rangle$ calculated by using the fact

$$\langle A \rangle = -\frac{\partial}{\partial \rho} g(\rho, t) \Big|_{\rho=0} \quad (52)$$

with $g(\rho, t) = G_1(\rho, t) + G_2(\rho, t)$. More specifically, after differentiating (17) w.r.t. ρ and setting $\rho = 0$, we then solve the system by the CIMs. At this time, one can check that the analytical domain of the new system is no smaller than the original one, therefore the discussions in above sections still work. See the simulation results in Figure 4.3, which further verifies the theoretical predictions.

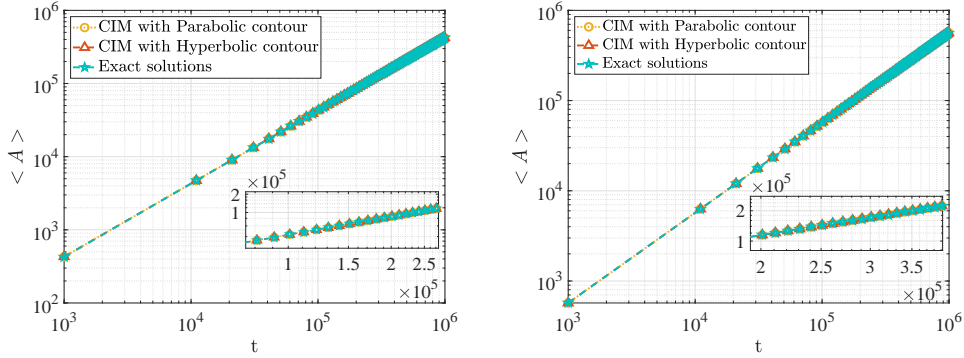


Figure 4.3: The simulations of $\langle A \rangle$ (in log-log scale); (left) $\langle A \rangle$ for the first internal state, i.e., $U(1) = 1, U(2) = 0$; (right) $\langle A \rangle$ for the second internal state, i.e., $U(1) = 0, U(2) = 1$. For both (left) and (right), we take $N = 100, \Lambda = 50, \alpha_1 = \alpha_2 = 0.5, G_{1,0} = 0.45, G_{2,0} = 0.55, \varepsilon_1 = 1/2, \varepsilon_2 = 1/2, t \in [1E + 3, 1E + 6]$.

5. Conclusions

The Feynman-Kac equation with two internal states describes the functional distribution of the particle's internal states. This paper presents the regularity analyses for the system, and built the CIMs with numerical stability analysis and error estimates. With the reference solutions provided by the time-marching schemes, the performances (of the CIMs) on spectral accuracy, low computational complexity, and small memory requirement, etc, are obtained. As one of the physical applications, by using the CIMs, we calculate the average occupation time of the first and second state of the stochastic process with two internal states.

Appendix A. The proofs of the results presented in Section 2.2

The techniques of the proofs are inspired by [26].

Appendix A.1. The proof of Lemma 2.1

PROOF. For $z \in \Sigma_{\theta, \delta}$, there is

$$\frac{|(z + \rho U(j))^{-\alpha_j}|}{|z|^{-\alpha_j}} = \left(\frac{|z|}{|z + \rho U(j)|} \right)^{\alpha_j} \leq \left(\frac{|z|}{|z| - |\rho U(j)|} \right)^{\alpha_j}.$$

Since $\delta > 2|\rho_s U(j)|$, it has

$$|z| - |\rho U(j)| \geq |z| - \frac{1}{2}|z| = \frac{1}{2}|z|.$$

Then

$$\frac{|(z + \rho U(j))^{-\alpha_j}|}{|z|^{-\alpha_j}} \leq (2)^{\alpha_j} \leq 2.$$

Appendix A.2. The proof of Lemma 2.2

PROOF. For $z \in \Sigma_{\theta, \delta}$, let

$$\left((z + \rho U(j))^{\alpha_j} - m_j B_{\alpha_j}^{-1} \right) u_j = v_j, \quad j = 1, 2.$$

Then

$$u_j = ((z + \rho U(j))^{\alpha_j})^{-1} v_j + m_j B_{\alpha_j}^{-1} ((z + \rho U(j))^{\alpha_j})^{-1} u_j, \quad j = 1, 2.$$

Taking modulus on both sides of the above equality and by Lemma 2.1, we have

$$|u_j| \leq \left| ((z + \rho U(j))^{\alpha_j})^{-1} \right| |v_j| + \left| m_j B_{\alpha_j}^{-1} ((z + \rho U(j))^{\alpha_j})^{-1} \right| |u_j| \leq 2|z|^{-\alpha_j} |v_j| + 2 \left| m_j B_{\alpha_j}^{-1} \right| |z|^{-\alpha_j} |u_j|, \quad j = 1, 2.$$

According to the condition that δ satisfies, there holds $2 \left| m_j B_{\alpha_j}^{-1} \right| |z|^{-\alpha_j} < \frac{1}{2}$. Thus,

$$|u_j| \leq 4|z|^{-\alpha_j} |v_j|, \quad j = 1, 2,$$

which implies the desired estimates.

Appendix A.3. The proof of Lemma 2.3

PROOF. For all $z \in \Sigma_{\theta, \delta}$, let

$$\left\{ \left((z + \rho U(1))^{\alpha_1} - m_1 B_{\alpha_1}^{-1} \right) \left((z + \rho U(2))^{\alpha_2} - m_2 B_{\alpha_2}^{-1} \right) - m_1 m_2 B_{\alpha_1}^{-1} B_{\alpha_2}^{-1} \right\} u = v.$$

After simple calculations, we have

$$\begin{aligned} u &= \left((z + \rho U(1))^{\alpha_1} - m_1 B_{\alpha_1}^{-1} \right)^{-1} \left((z + \rho U(2))^{\alpha_2} - m_2 B_{\alpha_2}^{-1} \right)^{-1} v \\ &\quad + m_1 m_2 B_{\alpha_1}^{-1} B_{\alpha_2}^{-1} \left((z + \rho U(1))^{\alpha_1} - m_1 B_{\alpha_1}^{-1} \right)^{-1} \left((z + \rho U(2))^{\alpha_2} - m_2 B_{\alpha_2}^{-1} \right)^{-1} u. \end{aligned}$$

Taking modulus on both sides of the above equality and by Lemma 2.2, there is

$$|u| \leq 16|z|^{-\alpha_1 - \alpha_2} |v| + 16 \left| m_1 m_2 B_{\alpha_1}^{-1} B_{\alpha_2}^{-1} \right| |z|^{-\alpha_1 - \alpha_2} |u|.$$

According to the condition that δ satisfies, there holds $16 \left| m_1 m_2 B_{\alpha_1}^{-1} B_{\alpha_2}^{-1} \right| |z|^{-\alpha_1 - \alpha_2} < \frac{1}{2}$. Thus,

$$|u| \leq 32|z|^{-\alpha_1 - \alpha_2} |v|,$$

which implies the desired estimate on $H(z)$.

For $H_{\alpha_1}(z)$, similarly, let

$$\left((z + \rho U(1))^{\alpha_1} - m_1 B_{\alpha_1}^{-1} \right) u = v + m_1 m_2 B_{\alpha_1}^{-1} B_{\alpha_2}^{-1} \left((z + \rho U(2))^{\alpha_2} - m_2 B_{\alpha_2}^{-1} \right)^{-1} u.$$

There exists

$$u = m_1 m_2 B_{\alpha_1}^{-1} B_{\alpha_2}^{-1} \left((z + \rho U(1))^{\alpha_1} - m_1 B_{\alpha_1}^{-1} \right)^{-1} \left((z + \rho U(2))^{\alpha_2} - m_2 B_{\alpha_2}^{-1} \right)^{-1} u + \left((z + \rho U(1))^{\alpha_1} - m_1 B_{\alpha_1}^{-1} \right)^{-1} v.$$

Taking modulus on both sides of the above equality and based on Lemma 2.2, there holds

$$|u| \leq 4|z|^{-\alpha_1} |v| + 16 |m_1 m_2 B_{\alpha_1}^{-1} B_{\alpha_2}^{-1}| |z|^{-\alpha_1 - \alpha_2} |u|.$$

According to the previous estimate, there is $16 |m_1 m_2 B_{\alpha_1}^{-1} B_{\alpha_2}^{-1}| |z|^{-\alpha_1 - \alpha_2} < \frac{1}{2}$. Thus,

$$|u| \leq 8|z|^{-\alpha_1} |v|,$$

which implies the desired estimate on $H_{\alpha_1}(z)$. By analogy, one can obtain the estimate on $H_{\alpha_2}(z)$.

Appendix A.4. The proof of Lemma 2.4

PROOF. According to the condition that δ satisfies and Lemma 2.1 and Lemma 2.3, the conclusions can be similarly obtained.

Appendix A.5. The proof of Theorem 2.1

PROOF. By the inverse Laplace transform, the solution in (11) is

$$G_1(t) = \frac{1}{2\pi i} \int_{\Gamma_{\theta, \delta}} e^{zt} \left(H_{\alpha_1}(z)(z + \rho U(1))^{\alpha_1 - 1} G_{1,0} - m_2 B_{\alpha_2}^{-1} H(z)(z + \rho U(1))^{\alpha_1 - 1} G_{2,0} \right) dz.$$

Taking q -th ($q = 0, 1$) derivative leads to

$$\frac{\partial^q}{\partial t^q} G_1(t) = \frac{1}{2\pi i} \int_{\Gamma_{\theta, \delta}} z^q e^{zt} \left(H_{\alpha_1}(z)(z + \rho U(1))^{\alpha_1 - 1} G_{1,0} - m_2 B_{\alpha_2}^{-1} H(z)(z + \rho U(1))^{\alpha_1 - 1} G_{2,0} \right) dz.$$

From Lemma 2.4, there exists

$$\begin{aligned} \left| \frac{\partial^q}{\partial t^q} G_1(t) \right| &= \left| \frac{1}{2\pi i} \int_{\Gamma_{\theta, \delta}} z^q e^{zt} \left(H_{\alpha_1}(z)(z + \rho U(1))^{\alpha_1 - 1} G_{1,0} - m_2 B_{\alpha_2}^{-1} H(z)(z + \rho U(1))^{\alpha_1 - 1} G_{2,0} \right) dz \right| \\ &\leq \frac{8}{\pi} \int_{\Gamma_{\theta, \delta}} e^{Re(z)t} |z|^{q-1} |G_{1,0}| |dz| + \frac{32 |m_2 B_{\alpha_2}^{-1}|}{\pi} \int_{\Gamma_{\theta, \delta}} e^{Re(z)t} |z|^{q-\alpha_2-1} |G_{2,0}| |dz| \\ &\leq \frac{8}{\pi} \left(\int_{\delta}^{+\infty} e^{rt \cos(\theta)} r^{q-1} dr + \int_{-\theta}^{\theta} e^{\delta t \cos(\varphi)} \delta^q d\varphi \right) |G_{1,0}| \\ &\quad + \frac{32 |m_2 B_{\alpha_2}^{-1}|}{\pi} \left(\int_{\delta}^{+\infty} e^{rt \cos(\theta)} r^{q-\alpha_2-1} dr + \int_{-\theta}^{\theta} e^{\delta t \cos(\varphi)} \delta^{q-\alpha_2} d\varphi \right) |G_{2,0}|. \end{aligned}$$

Let $rt = s$. Since $t > 1/\delta$, there exists

$$\begin{aligned} \left| \frac{\partial^q}{\partial t^q} G_1(t) \right| &\leq \frac{8}{\pi} \left(t^{-q} \int_1^{+\infty} e^{s \cos(\theta)} s^{q-1} ds + \delta^q \int_{-\theta}^{\theta} e^{\delta t \cos(\varphi)} d\varphi \right) |G_{1,0}| \\ &\quad + \frac{32 |m_2 B_{\alpha_2}^{-1}|}{\pi} \left(t^{\alpha_2 - q} \int_1^{+\infty} e^{s \cos(\theta)} s^{q-\alpha_2-1} ds + \delta^{q-\alpha_2} \int_{-\theta}^{\theta} e^{\delta t \cos(\varphi)} d\varphi \right) |G_{2,0}| \\ &\leq \frac{8}{\pi} \left((-1/\cos(\theta)) t^{-q} e^{\cos(\theta)} + 2\theta \delta^q e^{\delta T} \right) |G_{1,0}| \\ &\quad + \frac{32 |m_2 B_{\alpha_2}^{-1}|}{\pi} \left((-1/\cos(\theta)) t^{\alpha_2 - q} e^{\cos(\theta)} + 2\theta \delta^{q-\alpha_2} e^{\delta T} \right) |G_{2,0}|. \end{aligned}$$

Similarly,

$$\left| G_2^{(q)}(t) \right| \leq \frac{32 |m_1 B_{\alpha_1}^{-1}|}{\pi} \left((-1/\cos(\theta)) t^{\alpha_1 - q} e^{\cos(\theta)} + 2\theta \delta^{q-\alpha_1} e^{\delta T} \right) |G_{1,0}| + \frac{8}{\pi} \left((-1/\cos(\theta)) t^{-q} e^{\cos(\theta)} + 2\theta \delta^q e^{\delta T} \right) |G_{2,0}|.$$

The proof is completed.

Appendix B. The proofs of the results presented in Section 3

Appendix B.1. The proof of Proposition 3.1

PROOF. Let the denominator of $H(z)$ be zero, i.e.,

$$((z + \rho U(1))^{\alpha_1} - C_1)((z + \rho U(2))^{\alpha_2} - C_2) - C_1 C_2 = 0. \quad (\text{B.1})$$

Denote $u_1 + iv_1 := (z + \rho U(1))^{\alpha_1}$, $u_2 + iv_2 := (z + \rho U(2))^{\alpha_2}$. Then (B.1) can be rewritten as

$$((u_1 - C_1)(u_2 - C_2) - v_1 v_2 - C_1 C_2) + i((u_1 - C_1)v_2 + (u_2 - C_2)v_1) = 0. \quad (\text{B.2})$$

In the sequence, we prove that if (23) holds, (B.2) does not hold.

We divide the proof into the following cases:

Case I: For the case $u_1 > 2C_1$ and $u_2 > 2C_2$, if $v_1 v_2 \leq 0$, then $(u_1 - C_1)(u_2 - C_2) - v_1 v_2 - C_1 C_2 \neq 0$; otherwise, $(u_1 - C_1)v_2 + (u_2 - C_2)v_1 \neq 0$.

Case II: For the case $|v_1| > |C_1|$ and $|v_2| > |C_2|$,

- (a) when $u_1 \leq 2C_1$ and $u_2 \leq 2C_2$: If $(u_1 - C_1)(u_2 - C_2) > 0$, for $v_1 v_2 > 0$, there is $(u_1 - C_1)v_2 + (u_2 - C_2)v_1 \neq 0$; for $v_1 v_2 < 0$, we have $(u_1 - C_1)(u_2 - C_2) - v_1 v_2 - C_1 C_2 \neq 0$. If $(u_1 - C_1)(u_2 - C_2) = 0$, $(u_1 - C_1)v_2 + (u_2 - C_2)v_1 \neq 0$. If $(u_1 - C_1)(u_2 - C_2) < 0$, for $v_1 v_2 > 0$, there is $(u_1 - C_1)(u_2 - C_2) - v_1 v_2 - C_1 C_2 \neq 0$; for $v_1 v_2 < 0$, we have $(u_1 - C_1)v_2 + (u_2 - C_2)v_1 \neq 0$.
- (b) when $(u_1 - 2C_1)(u_2 - 2C_2) \leq 0$: If $(u_1 - C_1)(u_2 - C_2) > 0$, for $v_1 v_2 > 0$, there is $(u_1 - C_1)v_2 + (u_2 - C_2)v_1 \neq 0$; for $v_1 v_2 < 0$, we have $(u_1 - C_1)(u_2 - C_2) - v_1 v_2 - C_1 C_2 \neq 0$. If $(u_1 - C_1)(u_2 - C_2) = 0$, there is $(u_1 - C_1)(u_2 - C_2) - v_1 v_2 - C_1 C_2 \neq 0$. If $(u_1 - C_1)(u_2 - C_2) < 0$, for $v_1 v_2 > 0$, there is $(u_1 - C_1)(u_2 - C_2) - v_1 v_2 - C_1 C_2 \neq 0$.

To sum up, when (23) holds, $H(z)$ is analytic.

Appendix B.2. The proof of (24)

PROOF. For the proof of (24), we split it into the following two cases:

Case I: Let $\text{Re}(z + \rho U(j)) > 0$, i.e., $\text{Re}(z) > -\text{Re}(\rho U(j))$. For fixed $0 < \alpha_j < 1$, there are $\theta_j := \arg(z + \rho U(j)) \in (-\frac{\pi}{2}, \frac{\pi}{2})$ and $\alpha_j \theta_j \in (-\frac{\alpha_j \pi}{2}, \frac{\alpha_j \pi}{2})$. Further, we have $\text{Re}((z + \rho U(j))^{\alpha_j}) = |z + \rho U(j)|^{\alpha_j} \cos(\alpha_j \theta_j) > |z + \rho U(j)|^{\alpha_j} \cos(\frac{\alpha_j \pi}{2})$. If $|z + \rho U(j)|^{\alpha_j} \cos(\frac{\alpha_j \pi}{2}) > 2|C_j|$, that is $|z + \rho U(j)| > (2|C_j|/\cos(\alpha_j \pi/2))^{1/\alpha_j}$, then $\text{Re}(z + \rho U(j)) = |z + \rho U(j)| \cos(\alpha_j \theta_j) > 2|C_j|/\cos(\alpha_j \pi/2))^{1/\alpha_j} \cos(\alpha_j \pi)$. Hence, denote

$$d_1^{(j)} := \left(2|C_j|/\cos(\alpha_j \pi/2)\right)^{1/\alpha_j} - \text{Re}(\rho U(j)), \quad j = 1, 2.$$

Once $\text{Re}(z) > d_1 := \max\{d_1^{(1)}, d_1^{(2)}\}$, there holds $\text{Re}((z + \rho U(j))^{\alpha_j}) > 2|C_j|$, $j = 1, 2$. By (23), $H(z)$ is analytic.

Case II: By (23), $H(z)$ is analytic if $|\text{Im}((z + \rho U(j))^{\alpha_j})| > |C_j|$ and $|\text{Re}((z + \rho U(j))^{\alpha_j})| \leq 2|C_j|$ at the same time. So, if $\text{Im}((z + \rho U(j))^{\alpha_j}) = |z + \rho U(j)|^{\alpha_j} \sin(\alpha_j \theta_j) > |z + \rho U(j)|^{\alpha_j} \sin((|C_j|^2/(5|C_j|^2))^{1/2}) > |C_j|$ (where θ_j are defined as above), i.e., $|z + \rho U(j)| > (\sqrt{5}|C_j|)^{1/\alpha_j}$, then $H(z)$ is analytic. With this, let $|z + \rho U(j)| > |\text{Im}(z + \rho U(j))| \geq ||\text{Im}(z)| - |\text{Im}(\rho U(j))|| > (\sqrt{5}|C_j|)^{1/\alpha_j}$, and denote

$$d_2^{(j)} := \left(\sqrt{5}|C_j|\right)^{1/\alpha_j} + |\text{Im}(\rho U(j))|, \quad j = 1, 2.$$

Then, for $|\text{Im}(z)| > d_2 := \max\{d_2^{(1)}, d_2^{(2)}\}$, there is $|\text{Im}((z + \rho U(j))^{\alpha_j})| > |C_j|$, and $H(z)$ is analytic.

Above all, if z satisfies the conditions in (24), then $H(z)$ is analytic.

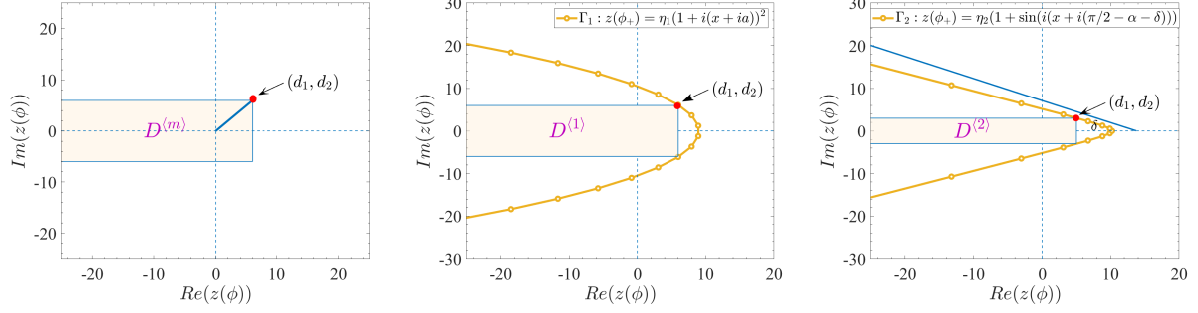


Figure B.1: Diagrammatic sketch for the condition (24) and the left boundary of $N^{(m)}$ for different integral contours. (left) is a domain determined by (24); (center) is to determine the parameters of the open strip $S^{(1)}$ when the CIM is with the parabolic contour Γ_1 ; (right) is to determine the parameters of the open strip $S^{(2)}$ when the CIM is with the hyperbolic contour Γ_2 .

Appendix B.3. Determination of the open strips $S^{(1)}$ and $S^{(2)}$

For strip $S^{(1)}$, which corresponds to the integral contour Γ_1 , as shown in Figure B.1 (center). Denote $\phi_+ := x + ia \in S$ with $a > 0$. Then

$$z(\phi_+) = \eta_1 \left((1 - a)^2 - x^2 \right) + 2i\eta_1 x(1 - a), \quad (\text{B.3})$$

$z(\phi_+) = z(x + ia)$ is the left boundary of $N^{(m)}$, which can be expressed as the parabola

$$u = \eta_1 \left((1 - a)^2 - \frac{v^2}{4\eta_1^2(1 - a)^2} \right), \quad (\text{B.4})$$

if denoting $z = u + iv$. As a increases from 0 to 1, the parabola (B.3) closes and reduces to the negative real axis. Hence, the left boundary of N_r determines the maximum value of a , which means that the parabola (B.4) passing through the point (d_1, d_2) , yields

$$a = 1 - \sqrt{\frac{d_1 + \sqrt{d_1^2 + d_2^2}}{2\eta_1}}, \quad (\text{B.5})$$

where d_1 and d_2 are given in Appendix B.2.

Denote $\phi_- := x - id$ with $d > 0$. The image of this horizontal line is

$$z(\phi_-) = \eta_1 \left((1 + d)^2 - x^2 \right) + 2i\eta_1 x(1 + d). \quad (\text{B.6})$$

As d away from 0, the parabola (B.6) widens and moves to the right. The optimal d and η_1 determined in (32) and (45), respectively.

For the strip $S^{(2)}$, which corresponds to the integral contour Γ_2 , as shown in Figure B.1 (right). From the expression of Γ_2 , the image of the horizontal line $\phi = x + iy$ is

$$z(\phi) = \eta_2 (1 - \sin(\alpha + y) \cosh(x)) + i\eta_2 \cos(\alpha + y) \sinh(x), \quad (\text{B.7})$$

which can be expressed as the hyperbola

$$\left(\frac{\eta_2 - u}{\sin(\alpha + y)} \right)^2 - \left(\frac{v}{\cos(\alpha + y)} \right)^2 = \eta_2^2, \quad (\text{B.8})$$

if denoting $z = u + iv$. As r increases from 0 to $r = \pi/2 - \alpha$, the left branch of parabola (B.7) closes and degenerates into the negative real axis. While, for $y < 0$, when r decreases from 0 to $-\alpha$, the hyperbola widens and becomes a vertical line. The minimum value of δ can be obtained by taking $z(\phi_+) := z(x + i(\pi/2 - \alpha - \delta))$ as the left boundary of $N^{(m)}$. More specifically, $z(\phi_+)$ can be expressed as a hyperbola with the asymptotes

$$v = \pm \tan(\delta)(\eta_2 - u), \quad (\text{B.9})$$

if denoting $z = u + iv$. Let one of the asymptotic lines $v = \tan(\delta)(\eta_2 - u)$ pass through the fixed point (d_1, d_2) , which results in $\delta = \arctan\left(\frac{d_2}{\eta_2 - d_1}\right)$. Besides, the optimal parameter α and η_2 are determined by maximizing $Q(\alpha) = \frac{\pi^2 - 2\pi\alpha - 2\pi\delta}{A(\alpha)}$ (see Subsection 3.2.3 and (47)). Then, the strip $S^{(2)}$ is determined.

Appendix B.4. The proof of Lemma 3.2

PROOF. For the first part of the lemma, as $z(\phi) = \eta_1(i\phi + 1)^2$ and $z'(\phi) = i2\eta_1(i\phi + 1)$, from the expression of $v_1(t, \phi)$, there is

$$v_1(t, \phi) = \frac{\eta_1}{\pi} e^{\eta_1(i\phi+1)^2 t} (1 + i\phi) \widehat{G}_1(\eta_1(1 + i\phi)^2) \quad \forall \phi \in S^{(1)}.$$

Choose $\phi_+ = x + iy \in S^{(1)}$, $0 < y < a < 1$, from the upper half plane of the strip $S^{(1)}$, for $t > 0$, there holds

$$v_1(t, x + iy) = \frac{\eta_1 e^{\eta_1((1-y)^2 - x^2)t}}{\pi} e^{i2\eta_1 t x(1-y)} (1 - y + ix) \widehat{G}_1(\eta_1(1 - y + ix)^2).$$

Taking the modulus of the left and right sides of the above formula leads to

$$|v_1(t, x + iy)| \leq \frac{\eta_1 e^{\eta_1(1-y)^2 t}}{\pi} e^{-x^2 \eta_1 t} \left| (1 - y + ix) \widehat{G}_1(\eta_1(1 - y + ix)^2) \right|.$$

Denote $l = 1 - y$, $l \in (1 - a, 1)$. From Lemma 2.4, there holds $|\widehat{G}_1(z)| \leq 16|z|^{-1}|G_{1,0}| + 64|m_1 B_{\alpha_1}^{-1}| |z|^{-1-\alpha_2}|G_{2,0}|$. With these, we have

$$\left| (l + ix) \widehat{G}_1(\eta_1(l + ix)^2) \right| \leq \left(\frac{16|l + ix|}{|\eta_1(l + ix)^2|} |G_{1,0}| + \frac{64|m_1 B_{\alpha_1}^{-1}| |l + ix|}{|\eta_1(l + ix)^2|^{1+\alpha_2}} |G_{2,0}| \right).$$

Since

$$\frac{|l + ix|}{|\eta_1(l + ix)^2|} \leq \frac{1}{\eta_1(1 - a)} \quad \text{and} \quad \frac{|l + ix|}{|\eta_1(l + ix)^2|^{1+\alpha_2}} \leq \frac{1}{\eta_1^{1+\alpha_2} (1 - a)^{1+2\alpha_2}},$$

we have

$$\begin{aligned} |v_1(t, x + iy)| &\leq \frac{\eta_1 e^{\eta_1 t}}{\pi} \left(\frac{16}{\eta_1(1 - a)} |G_{1,0}| + \frac{64|m_1 B_{\alpha_1}^{-1}|}{\eta_1^{1+\alpha_2} (1 - a)^{1+2\alpha_2}} |G_{2,0}| \right) e^{-\eta_1 t x^2} \\ &\leq \frac{e^{\eta_1 t}}{\pi} \max \left\{ 16(1 - a)^{-1}, 64|m_1 B_{\alpha_1}^{-1}| (1 - a)^{-(1+2\alpha_2)} \right\} (|G_{1,0}| + \eta_1^{-\alpha_2} |G_{2,0}|) e^{-\eta_1 t x^2}. \end{aligned}$$

Choose $\phi_- = x - iy \in S^{(1)}$, $-d < -y$, from the lower half plane of $S^{(1)}$, for $t > 0$, there holds

$$\begin{aligned} |v_1(t, x - iy)| &\leq \frac{\eta_1 e^{\eta_1(1+d)^2 t}}{\pi} (16\eta_1^{-1} |G_{1,0}| + 64|m_1 B_{\alpha_1}^{-1}| \eta_1^{-(1+\alpha_2)} |G_{2,0}|) e^{-\eta_1 t x^2} \\ &\leq \frac{e^{\eta_1 t}}{\pi} \max \left\{ 16e^{(2d+d^2)\eta_1 t}, 64|m_1 B_{\alpha_1}^{-1}| e^{(2d+d^2)\eta_1 t} \right\} (|G_{1,0}| + \eta_1^{-\alpha_2} |G_{2,0}|) e^{-\eta_1 t x^2}. \end{aligned}$$

Therefore, for $\phi \in S^{(1)}$, by denoting

$$B := \max \left\{ 16(1 - a)^{-1}, 64|m_1 B_{\alpha_1}^{-1}| (1 - a)^{-(1+2\alpha_2)}, 16e^{(2d+d^2)\eta_1 t}, 64|m_1 B_{\alpha_1}^{-1}| e^{(2d+d^2)\eta_1 t} \right\}, \quad (\text{B.10})$$

we have

$$|v_1(t, \phi)| \leq \frac{B e^{\eta_1 t}}{\pi} (|G_{1,0}| + \eta_1^{-\alpha_2} |G_{2,0}|) e^{-\eta_1 t x^2}.$$

For the case of $S^{(2)}$, the proof is similar to the previous one. Hence $v_1(t, \phi)$ is analytical in the strip $S^{(2)}$ and $z'(\phi) = i\eta_2 \cos(i\phi - \alpha)$. By choosing $\phi_+ = x + iy \in S^{(2)}$, $0 < y < \pi/2 - \delta - \alpha$, from the upper half plane of the strip $S^{(2)}$, for $t > 0$, there holds

$$v_1(t, x + iy) = \frac{\eta_2}{2\pi} e^{\eta_2(1 - \sin(\alpha + y - ix))t} \cos(\alpha + y - ix) \widehat{G}_1(\eta_2(1 - \sin(\alpha + y - ix))).$$

Denote $l' = \alpha + y$, $l' \in (\alpha, \pi/2 - \delta)$. After taking the modulus of the left and right sides of the above formula, we get

$$|v_1(t, x + ir)| \leq \frac{\eta_2}{2\pi} e^{\eta_2 t(1 - \sin l' \cosh x)} \left| \cos(l' - ix) \widehat{G}_1(\eta_2(1 - \sin(l' - ix))) \right|.$$

Moreover, since

$$\begin{aligned} \left| \cos(l' - ix) \widehat{G}_1(\eta_2(1 - \sin(l' - ix))) \right| &\leq \frac{16 |\cos(l' - ix)|}{|\eta_2(1 - \sin(l' - ix))|} |G_{1,0}| + \frac{64 |m_1 B_{\alpha_1}^{-1}| |\cos(l' - ix)|}{|(\eta_2(1 - \sin(l' - ix)))^{1+\alpha_2}|} |G_{2,0}|, \\ \frac{|\cos(l' - ix)|}{|\eta_2(1 - \sin(l' - ix))|} &\leq \frac{1}{\eta_2} \sqrt{\frac{1 + \sin l'}{1 - \sin l'}}, \end{aligned}$$

and

$$\begin{aligned} \frac{|\cos(l' - ix)|}{|(\eta_2(1 - \sin(l' - ix)))^{1+\alpha_2}|} &= \frac{1}{|(\eta_2(1 - \sin(l' - ix)))^{\alpha_2}|} \frac{|\cos(l' - ix)|}{|\eta_2(1 - \sin(l' - ix))|} \\ &\leq \frac{1}{\eta_2^{1+\alpha_2} (\cosh(x) - \sin l')^{\alpha_2}} \sqrt{\frac{1 + \sin l'}{1 - \sin l'}}, \end{aligned}$$

then, by $\sin \alpha < \sin l' = \sin(\alpha + y)$, there holds

$$|v_1(t, x + ir)| \leq \frac{8e^{\eta_2 t}}{\pi} \sqrt{\frac{1 + \sin(\alpha + y)}{1 - \sin(\alpha + y)}} \left(|G_{1,0}| + \frac{4 |m_1 B_{\alpha_1}^{-1}|}{\eta_2^{\alpha_2} (1 - \sin(\alpha + y))^{\alpha_2}} |G_{2,0}| \right) e^{-\eta_2 t \sin \alpha \cosh x}.$$

Choosing $\phi_- = x - iy \in S^{(2)}$, $-\alpha < -y$, from the lower half plane of $S^{(2)}$, for $t > 0$, we deduce

$$|v_1(t, x - iy)| \leq \frac{8e^{\eta_2 t}}{\pi} \sqrt{\frac{1 + \sin(\alpha + y)}{1 - \sin(\alpha + y)}} \left(|G_{1,0}| + \frac{4 |m_1 B_{\alpha_1}^{-1}|}{\eta_2^{\alpha_2} (1 - \sin(\alpha + y))^{\alpha_2}} |G_{2,0}| \right) e^{-\eta_2 t \sin \alpha \cosh x}.$$

Therefore, for $\phi \in S^{(2)}$, $0 < y < \min\{\alpha, \pi/2 - \alpha - \delta\}$, there holds

$$|v_1(t, \phi)| \leq \frac{8e^{\eta_2 t}}{\pi} \sqrt{\frac{1 + \sin(\alpha + y)}{1 - \sin(\alpha + y)}} \left(|G_{1,0}| + \frac{4 |m_1 B_{\alpha_1}^{-1}|}{\eta_2^{\alpha_2} (1 - \sin(\alpha + y))^{\alpha_2}} |G_{2,0}| \right) e^{-\eta_2 t \sin \alpha \cosh x}.$$

Similar estimates for $v_2(t, \phi)$ can be obtained on the strips $S^{(1)}$ and $S^{(2)}$, respectively.

Appendix B.5. The proof of Theorem 3.1

PROOF. We firstly choose the integral contour $z(\phi)$ as defined in (18) with the uniform step-size h_1 . For $t > 0$, by (25), there holds

$$|G_{1,N}^{(1)}(t)| \leq h_1 \sum_{|k| \leq N-1} |v_1(t, kh_1)| \leq \frac{2\eta_1 B e^{\eta_1 t}}{\pi} (\eta_1^{-1} |G_{1,0}| + \eta_1^{-(1+\alpha_2)} |G_{2,0}|) \int_0^{(N-1)h_1} e^{-x^2 \eta_1 t} dx.$$

Since

$$\int_0^{(N-1)h_1} e^{-x^2 \eta_1 t} dx \leq \int_0^\infty e^{-x^2 \eta_1 t} dx = \frac{\sqrt{\eta_1 t \pi}}{2\eta_1 t},$$

the result of the first part of the theorem holds.

For the rest part of this theorem, we choose the hyperbolic integral contour $z(\phi)$ defined in (19) with the uniform step-size h_2 . For $t > 0$ and $h_2 > 0$, by (26), there holds

$$\begin{aligned} |G_{1,N}^{(2)}(t)| &\leq h_2 \sum_{|k| \leq N-1} |v_1(t, kh_2)| \\ &\leq \frac{16e^{\eta_2 t}}{\pi} \sqrt{\frac{1 + \sin(\alpha + r)}{1 - \sin(\alpha + r)}} \left(|G_{1,0}| + \frac{4 |m_1 B_{\alpha_1}^{-1}|}{\eta_2^{\alpha_2} (1 - \sin(\alpha + r))^{\alpha_2}} |G_{2,0}| \right) \int_0^{(N-1)h_2} e^{-\eta_2 t \sin \alpha \cosh x} dx. \end{aligned}$$

Thanks to Lemma 3.1, there holds

$$\int_0^{(N-1)h_2} e^{-\eta_2 \sin(\alpha) \cosh(x)t} dx \leq \int_0^\infty e^{-\eta_2 \sin(\alpha) \cosh(x)t} dx \leq L(\eta_2 t \sin(\alpha)).$$

Similarly, we can obtain the stability results about $G_{2,N}^{(m)}(t)$, $m = 1, 2$.

Appendix C. The time-marching schemes for the Feynman-Kac system (Subsection 3.3)

Here we provide the time-marching schemes for (12) directly. To make things clear for readers, here we demonstrate them in a tedious way. After integrating from 0 to t on the left and right sides of (12), according to (48), for $t = t_{n+1}$, $n = 0, 1, \dots, M$, there hold

$$\begin{aligned} G_1(t_{n+1}) = & \frac{m_1 B_{\alpha_1}^{-1}}{\Gamma(\alpha_1)} \left(\int_0^{t_{n+1}} \frac{e^{-\rho U(1)(t_{n+1}-\tau)}}{(t_{n+1}-\tau)^{1-\alpha_1}} G_1(\tau) d\tau + (\rho U(1))^{1-\alpha_1} \gamma(\alpha_1, 1) \int_0^{t_{n+1}} G_1(\tau) d\tau \right) \\ & - \frac{m_2 B_{\alpha_2}^{-1}}{\Gamma(\alpha_2)} \left(\int_0^{t_{n+1}} \frac{e^{-\rho U(2)(t_{n+1}-\tau)}}{(t_{n+1}-\tau)^{1-\alpha_2}} G_2(\tau) d\tau + (\rho U(2))^{1-\alpha_2} \gamma(\alpha_2, 1) \int_0^{t_{n+1}} G_2(\tau) d\tau \right) \\ & - \rho U(1) \int_0^{t_{n+1}} G_1(\tau) d\tau + G_{1,0}, \end{aligned} \quad (C.1)$$

$$\begin{aligned} G_2(t_{n+1}) = & \frac{m_2 B_{\alpha_2}^{-1}}{\Gamma(\alpha_2)} \left(\int_0^{t_{n+1}} \frac{e^{-\rho U(2)(t_{n+1}-\tau)}}{(t_{n+1}-\tau)^{1-\alpha_2}} G_2(\tau) d\tau + (\rho U(2))^{1-\alpha_2} \gamma(\alpha_2, 1) \int_0^{t_{n+1}} G_2(\tau) d\tau \right) \\ & - \frac{m_1 B_{\alpha_1}^{-1}}{\Gamma(\alpha_1)} \left(\int_0^{t_{n+1}} \frac{e^{-\rho U(1)(t_{n+1}-\tau)}}{(t_{n+1}-\tau)^{1-\alpha_1}} G_1(\tau) d\tau + (\rho U(1))^{1-\alpha_1} \gamma(\alpha_1, 1) \int_0^{t_{n+1}} G_1(\tau) d\tau \right) \\ & - \rho U(2) \int_0^{t_{n+1}} G_2(\tau) d\tau + G_{2,0}, \end{aligned} \quad (C.2)$$

where $\gamma(\alpha_j, 1)$, $j = 1, 2$ are the incomplete Gamma function. With these, by the technics mentioned in [14], one can obtain the following numerical schemes.

Case I: For $n = 0$,

$$\begin{aligned} G_1(t_1) = & \frac{m_1 B_{\alpha_1}^{-1}}{\Gamma(\alpha_1)} \left(\frac{h^{\alpha_1}}{\alpha_1(\alpha_1 + 1)} \alpha_1 e^{-\rho U(1)h} + \frac{h}{2} (\rho U(1))^{1-\alpha_1} \gamma(\alpha_1, 1) \right) G_{1,0} \\ & + \frac{m_1 B_{\alpha_1}^{-1}}{\Gamma(\alpha_1)} \left(\frac{h^{\alpha_1}}{\alpha_1(\alpha_1 + 1)} + \frac{h}{2} (\rho U(1))^{1-\alpha_1} \gamma(\alpha_1, 1) \right) G_1(t_1) \\ & - \frac{m_2 B_{\alpha_2}^{-1}}{\Gamma(\alpha_2)} \left(\frac{h^{\alpha_2}}{\alpha_2(\alpha_2 + 1)} \alpha_2 e^{-\rho U(2)h} + \frac{h}{2} (\rho U(2))^{1-\alpha_2} \gamma(\alpha_2, 1) \right) G_{2,0} \\ & - \frac{m_2 B_{\alpha_2}^{-1}}{\Gamma(\alpha_2)} \left(\frac{h^{\alpha_2}}{\alpha_2(\alpha_2 + 1)} + \frac{h}{2} (\rho U(2))^{1-\alpha_2} \gamma(\alpha_2, 1) \right) G_2(t_1) \\ & - \frac{\rho U(1)h - 2}{2} G_{1,0} - \frac{\rho U(1)h}{2} G_1(t_1), \end{aligned} \quad (C.3)$$

$$\begin{aligned}
G_2(t_1) &= \frac{m_2 B_{\alpha_2}^{-1}}{\Gamma(\alpha_2)} \left(\frac{h^{\alpha_2}}{\alpha_2(\alpha_2 + 1)} \alpha_2 e^{-\rho U(2)h} + \frac{h}{2} (\rho U(2))^{1-\alpha_2} \gamma(\alpha_2, 1) \right) G_{2,0} \\
&\quad + \frac{m_2 B_{\alpha_2}^{-1}}{\Gamma(\alpha_2)} \left(\frac{h^{\alpha_2}}{\alpha_2(\alpha_2 + 1)} + \frac{h}{2} (\rho U(2))^{1-\alpha_2} \gamma(\alpha_2, 1) \right) G_2(t_1) \\
&\quad - \frac{m_1 B_{\alpha_1}^{-1}}{\Gamma(\alpha_1)} \left(\frac{h^{\alpha_1}}{\alpha_1(\alpha_1 + 1)} \alpha_1 e^{-\rho U(1)h} + \frac{h}{2} (\rho U(1))^{1-\alpha_1} \gamma(\alpha_1, 1) \right) G_{1,0} \\
&\quad - \frac{m_1 B_{\alpha_1}^{-1}}{\Gamma(\alpha_1)} \left(\frac{h^{\alpha_1}}{\alpha_1(\alpha_1 + 1)} + \frac{h}{2} (\rho U(1))^{1-\alpha_1} \gamma(\alpha_1, 1) \right) G_1(t_1) \\
&\quad - \frac{\rho U(2)h - 2}{2} G_{2,0} - \frac{\rho U(2)h}{2} G_2(t_1).
\end{aligned} \tag{C.4}$$

Denote

$$\begin{aligned}
a_{11} &= \frac{m_1 B_{\alpha_1}^{-1}}{\Gamma(\alpha_1)} \left(\frac{h^{\alpha_1}}{\alpha_1(\alpha_1 + 1)} + \frac{h}{2} (\rho U(1))^{1-\alpha_1} \gamma(\alpha_1, 1) \right) - \frac{\rho U(1)h}{2}, \\
a_{12} &= -\frac{m_2 B_{\alpha_2}^{-1}}{\Gamma(\alpha_2)} \left(\frac{h^{\alpha_2}}{\alpha_2(\alpha_2 + 1)} + \frac{h}{2} (\rho U(2))^{1-\alpha_2} \gamma(\alpha_2, 1) \right), \\
a_{21} &= -\frac{m_1 B_{\alpha_1}^{-1}}{\Gamma(\alpha_1)} \left(\frac{h^{\alpha_1}}{\alpha_1(\alpha_1 + 1)} + \frac{h}{2} (\rho U(1))^{1-\alpha_1} \gamma(\alpha_1, 1) \right), \\
a_{22} &= \frac{m_2 B_{\alpha_2}^{-1}}{\Gamma(\alpha_2)} \left(\frac{h^{\alpha_2}}{\alpha_2(\alpha_2 + 1)} + \frac{h}{2} (\rho U(2))^{1-\alpha_2} \gamma(\alpha_2, 1) \right) - \frac{\rho U(2)h}{2},
\end{aligned}$$

and

$$\begin{aligned}
b_1^{(0)} &= \frac{m_1 B_{\alpha_1}^{-1}}{\Gamma(\alpha_1)} \left(\frac{h^{\alpha_1}}{\alpha_1(\alpha_1 + 1)} \alpha_1 e^{-\rho U(1)h} + \frac{h}{2} (\rho U(1))^{1-\alpha_1} \gamma(\alpha_1, 1) \right) G_{1,0} - \frac{\rho U(1)h - 2}{2} G_{1,0} \\
&\quad - \frac{m_2 B_{\alpha_2}^{-1}}{\Gamma(\alpha_2)} \left(\frac{h^{\alpha_2}}{\alpha_2(\alpha_2 + 1)} \alpha_2 e^{-\rho U(2)h} + \frac{h}{2} (\rho U(2))^{1-\alpha_2} \gamma(\alpha_2, 1) \right) G_{2,0}, \\
b_2^{(0)} &= \frac{m_2 B_{\alpha_2}^{-1}}{\Gamma(\alpha_2)} \left(\frac{h^{\alpha_2}}{\alpha_2(\alpha_2 + 1)} \alpha_2 e^{-\rho U(2)h} + \frac{h}{2} (\rho U(2))^{1-\alpha_2} \gamma(\alpha_2, 1) \right) G_{2,0} - \frac{\rho U(2)h - 2}{2} G_{2,0} \\
&\quad - \frac{m_1 B_{\alpha_1}^{-1}}{\Gamma(\alpha_1)} \left(\frac{h^{\alpha_1}}{\alpha_1(\alpha_1 + 1)} \alpha_1 e^{-\rho U(1)h} + \frac{h}{2} (\rho U(1))^{1-\alpha_1} \gamma(\alpha_1, 1) \right) G_{1,0}.
\end{aligned}$$

Then, there holds

$$\begin{bmatrix} 1 & 0 \\ 0 & 1 \end{bmatrix} \begin{bmatrix} G_1(t_1) \\ G_2(t_1) \end{bmatrix} = \begin{bmatrix} b_1^{(0)} \\ b_2^{(0)} \end{bmatrix} + \begin{bmatrix} a_{11} & a_{12} \\ a_{21} & a_{22} \end{bmatrix} \cdot \begin{bmatrix} G_1(t_1) \\ G_2(t_1) \end{bmatrix}.$$

Furthermore, we can obtain that

$$\begin{bmatrix} G_1(t_1) \\ G_2(t_1) \end{bmatrix} = \begin{bmatrix} 1 - a_{11} & -a_{12} \\ -a_{21} & 1 - a_{22} \end{bmatrix}^{-1} \cdot \begin{bmatrix} b_1^{(0)} \\ b_2^{(0)} \end{bmatrix}. \tag{C.5}$$

Since the matrix $\begin{bmatrix} 1 - a_{11} & -a_{12} \\ -a_{21} & 1 - a_{22} \end{bmatrix}$ is a principally diagonally dominant matrix, so it is invertible.

Case II: For $n \geq 1$, there are

$$\begin{aligned}
G_1(t_{n+1}) &= \frac{m_1 B_{\alpha_1}^{-1}}{\Gamma(\alpha_1)} \left(\frac{h^{\alpha_1}}{\alpha_1(\alpha_1 + 1)} \sum_{j=0}^n d_{j,n}^{(1)} G_1(t_j) + (\rho U(1))^{1-\alpha_1} \gamma(\alpha_1, 1) \left(\frac{h}{2} G_{1,0} + h \sum_{j=1}^n G_1(t_j) \right) \right) \\
&\quad + \frac{m_1 B_{\alpha_1}^{-1}}{\Gamma(\alpha_1)} \left(\frac{h^{\alpha_1}}{\alpha_1(\alpha_1 + 1)} + \frac{h}{2} (\rho U(1))^{1-\alpha_1} \gamma(\alpha_1, 1) \right) G_1(t_{n+1})
\end{aligned}$$

$$\begin{aligned}
& - \frac{m_2 B_{\alpha_2}^{-1}}{\Gamma(\alpha_2)} \left(\frac{h^{\alpha_2}}{\alpha_2(\alpha_2 + 1)} \sum_{j=0}^n d_{j,n}^{(2)} G_2(t_j) + (\rho U(2))^{1-\alpha_2} \gamma(\alpha_2, 1) \left(\frac{h}{2} G_{2,0} + h \sum_{j=1}^n G_2(t_j) \right) \right) \\
& - \frac{m_2 B_{\alpha_2}^{-1}}{\Gamma(\alpha_2)} \left(\frac{h^{\alpha_2}}{\alpha_2(\alpha_2 + 1)} + \frac{h}{2} (\rho U(2))^{1-\alpha_2} \gamma(\alpha_2, 1) \right) G_2(t_{n+1}) \\
& - \rho U(1) \left(\frac{h}{2} G_{1,0} + h \sum_{j=1}^n G_1(t_j) \right) - \frac{\rho U(1)h}{2} G_1(t_{n+1}) + G_{1,0}
\end{aligned}$$

and

$$\begin{aligned}
G_2(t_{n+1}) &= \frac{m_2 B_{\alpha_2}^{-1}}{\Gamma(\alpha_2)} \left(\frac{h^{\alpha_2}}{\alpha_2(\alpha_2 + 1)} \sum_{j=0}^n d_{j,n}^{(2)} G_2(t_j) + (\rho U(2))^{1-\alpha_2} \gamma(\alpha_2, 1) \left(\frac{h}{2} G_{2,0} + h \sum_{j=1}^n G_2(t_j) \right) \right) \\
&+ \frac{m_2 B_{\alpha_2}^{-1}}{\Gamma(\alpha_2)} \left(\frac{h^{\alpha_2}}{\alpha_2(\alpha_2 + 1)} + \frac{h}{2} (\rho U(2))^{1-\alpha_2} \gamma(\alpha_2, 1) \right) G_2(t_{n+1}) \\
&- \frac{m_1 B_{\alpha_1}^{-1}}{\Gamma(\alpha_1)} \left(\frac{h^{\alpha_1}}{\alpha_1(\alpha_1 + 1)} \sum_{j=0}^n d_{j,n}^{(1)} G_1(t_j) + (\rho U(1))^{1-\alpha_1} \gamma(\alpha_1, 1) \left(\frac{h}{2} G_{1,0} + h \sum_{j=1}^n G_1(t_j) \right) \right) \\
&- \frac{m_1 B_{\alpha_1}^{-1}}{\Gamma(\alpha_1)} \left(\frac{h^{\alpha_1}}{\alpha_1(\alpha_1 + 1)} + \frac{h}{2} (\rho U(1))^{1-\alpha_1} \gamma(\alpha_1, 1) \right) G_1(t_{n+1}) \\
&- \rho U(1) \left(\frac{h}{2} G_{2,0} + h \sum_{j=1}^n G_2(t_j) \right) - \frac{\rho U(1)h}{2} G_2(t_{n+1}) + G_{2,0},
\end{aligned}$$

where

$$d_{j,n}^{(m)} = \begin{cases} e^{-\rho U(m)(n+1)h} (n^{\alpha_m+1} - (n+1)^{\alpha_m} (n - \alpha_m)), & \text{if } j = 0, \\ e^{-\rho U(m)(n-j+1)h} ((n-j+2)^{\alpha_m+1} + (n-j)^{\alpha_m+1} - 2(n-j+1)^{\alpha_m+1}), & \text{if } 1 \leq j \leq n. \end{cases}, \quad m = 1, 2. \quad (\text{C.6})$$

Denote

$$\begin{aligned}
b_1^{(n)} &= \frac{m_1 B_{\alpha_1}^{-1}}{\Gamma(\alpha_1)} \left(\frac{h^{\alpha_1}}{\alpha_1(\alpha_1 + 1)} \sum_{j=0}^n d_{j,n}^{(1)} G_1(t_j) + (\rho U(1))^{1-\alpha_1} \gamma(\alpha_1, 1) \left(\frac{h}{2} G_{1,0} + h \sum_{j=1}^n G_1(t_j) \right) \right) \\
&- \frac{m_2 B_{\alpha_2}^{-1}}{\Gamma(\alpha_2)} \left(\frac{h^{\alpha_2}}{\alpha_2(\alpha_2 + 1)} \sum_{j=0}^n d_{j,n}^{(2)} G_2(t_j) + (\rho U(2))^{1-\alpha_2} \gamma(\alpha_2, 1) \left(\frac{h}{2} G_{2,0} + h \sum_{j=1}^n G_2(t_j) \right) \right) \\
&- \rho U(1) \left(\frac{h}{2} G_{1,0} + h \sum_{j=1}^n G_1(t_j) \right) + G_{1,0},
\end{aligned}$$

and

$$\begin{aligned}
b_2^{(n)} &= \frac{m_2 B_{\alpha_2}^{-1}}{\Gamma(\alpha_2)} \left(\frac{h^{\alpha_2}}{\alpha_2(\alpha_2 + 1)} \sum_{j=0}^n d_{j,n}^{(2)} G_2(t_j) + (\rho U(2))^{1-\alpha_2} \gamma(\alpha_2, 1) \left(\frac{h}{2} G_{2,0} + h \sum_{j=1}^n G_2(t_j) \right) \right) \\
&- \frac{m_1 B_{\alpha_1}^{-1}}{\Gamma(\alpha_1)} \left(\frac{h^{\alpha_1}}{\alpha_1(\alpha_1 + 1)} \sum_{j=0}^n d_{j,n}^{(1)} G_1(t_j) + (\rho U(1))^{1-\alpha_1} \gamma(\alpha_1, 1) \left(\frac{h}{2} G_{1,0} + h \sum_{j=1}^n G_1(t_j) \right) \right) \\
&- \rho U(2) \left(\frac{h}{2} G_{2,0} + h \sum_{j=1}^n G_2(t_j) \right) + G_{2,0}.
\end{aligned}$$

Thus,

$$\begin{bmatrix} G_1(t_{n+1}) \\ G_2(t_{n+1}) \end{bmatrix} = \begin{bmatrix} 1 - a_{11} & -a_{12} \\ -a_{21} & 1 - a_{22} \end{bmatrix}^{-1} \cdot \begin{bmatrix} b_1^{(n)} \\ b_2^{(n)} \end{bmatrix}, \quad n = 1, 2, \dots, M. \quad (\text{C.7})$$

Combining (C.5) with (C.7), the time marching scheme for system (11) is obtained.

Acknowledgments

The authors Ma and Deng are supported by the National Natural Science Foundation of China under Grant No. 12071195, the AI and Big Data Funds under Grant No. 2019620005000775, and the Innovative Groups of Basic Research in Gansu Province under Grant No. 22JR5RA391. The author Zhao is supported by Guangdong Basic and Applied Basic Research Foundation under Grant No. 2022A1515011332. The authors have no relevant financial or non-financial interests to disclose.

References

References

- [1] A. Talbot, The accurate numerical inversion of Laplace transforms, *IMA J. Appl. Math.*, 23 (1979), 97-120.
- [2] B. Y. Li and S. Ma, Exponential convolution quadrature for nonlinear subdiffusion equations with nonsmooth initial data, *SIAM J. Numer. Anal.*, 60 (2022), 503-528.
- [3] B. Y. Li and S. Ma, A high-order exponential integrator for nonlinear parabolic equations with nonsmooth initial data, *J. Sci. Comput.*, 87 (2021), pp. 1-16.
- [4] B. Y. Li, Y. P. Lin, S. Ma, Q. Q. Rao, An exponential spectral method using VP means for semilinear subdiffusion equations with rough data, *SIAM J. Numer. Anal.*, 2023 (accepted).
- [5] B. Dingfelder and J. A. C. Weideman, An improved Talbot method for numerical Laplace transform inversion, *Numer. Algorithms*, 68 (2015), 167-183.
- [6] B. T. Jin, B. Y. Li, and Z. Zhou, Numerical analysis of nonlinear subdiffusion equations, *SIAM J. Numer. Anal.*, 56 (2018), 1-23.
- [7] D. Sheen, I. H. Sloan, and V. Thomée, A parallel method for time-discretization of parabolic problems based on contour integral representation and quadrature, *Math. Comp.*, 69 (2000), 177-195.
- [8] F. G. Ma, L. J. Zhao, W. H. Deng, and Y. J. Wang, Analyses of the contour integral method for time fractional subdiffusion-normal transport equation. [arXiv:2210.09594v1](https://arxiv.org/abs/2210.09594v1).
- [9] H. Zhang, F. H. Zeng, X. Y. Jiang, and G. E. Karniadakis, Convergence analysis of the time-stepping numerical methods for time-fractional nonlinear subdiffusion equations, *Fract. Calc. Appl. Anal.*, 25 (2022), 453-487.
- [10] H. Wang, R. E. Ewing, and T. F. Russell, Eulerian-Lagrangian localized adjoint methods for convection-diffusion equations and their convergence analysis, *IMA J. Numer. Anal.*, 15 (1995), 405-459.
- [11] I. Podlubny, *Fractional Differential Equations*, Academic Press, San Diego, 1999.
- [12] J. Lee and D. Sheen, A parallel method for backward parabolic problems based on the Laplace transformation, *SIAM J. Numer. Anal.*, 44 (2006), 1466-1486.
- [13] J. A. C. Weideman and L. N. Trefethen, Parabolic and hyperbolic contours for computing the Bromwich integral, *Math. Comp.*, 76 (2007), 1341-1356.
- [14] K. Diethelm, N. J. Ford, and A. D. Freed, A predictor-corrector approach for the numerical solution of fractional differential equations, *Nonlinear Dynam.*, 29 (2002), 3-22.
- [15] K. J. In't Hout and J. A. C. Weideman, A contour integral method for the Black-Scholes and Heston equations, *SIAM J. Sci. Comput.*, 33 (2011), 763-785.
- [16] L. N. Trefethen and J. A. C. Weideman, The exponentially convergent trapezoidal rule, *SIAM Rev.*, 56 (2014), 385-458.
- [17] L. J. Zhao, W. H. Deng, and J. S. Hethcote, Characterization of image spaces of riemann-liouville fractional integral operators on sobolev spaces $W^{m,p}(\Omega)$, *Sci. China Math.*, 64 (2021), 2611-2636.
- [18] M. L. Fernández and C. Palencia, On the numerical inversion of the Laplace transform of certain holomorphic mappings, *Appl. Numer. Math.*, 51 (2004), 289-303.
- [19] M. L. Fernández, C. Palencia, and A. Schädle, A spectral order method for inverting sectorial Laplace transforms, *SIAM J. Numer. Anal.*, 44 (2006), 1332-1350.
- [20] O. Taiwo, J. Schultz, and V. Krebs, A comparison of two methods for the numerical inversion of Laplace transforms, *Comput. Chem. Eng.*, 19 (1995), 303-308.
- [21] P. B. Xu and W. H. Deng, Fractional compound Poisson process with multiple internal states, *Math. Model. Nat. Phenom.*, 13 (2018), 10.
- [22] R. Piessens, A bibliography on numerical inversion of the Laplace transform and applications, *J. Comput. Appl. Math.*, 1 (1975), 115-128.
- [23] R. Piessens and N. D. P. Dang, A bibliography on numerical inversion of the Laplace transform and applications: A supplement, *J. Comput. Appl. Math.*, 2 (1976), 225-228.
- [24] S. Carmi, L. Turgeman, and E. Barkai, On distributions of functionals of anomalous diffusion paths, *J. Stat. Phys.*, 141 (2010), 1071-1092.
- [25] W. H. Deng, Short memory principle and a predictor-corrector approach for fractional differential equations, *J. Comput. Appl. Math.*, 206 (2007), 174-188.
- [26] W. H. Deng, B. Y. Li, Z. Qian, and H. Wang, Time discretization of a tempered fractional Feynman-Kac equation with measure data, *SIAM J. Numer. Anal.*, 56 (2018), 3249-3275.
- [27] W. McLean, I. H. Sloan, and V. Thomée, Time discretization via Laplace transformation of an integro-differential equation of parabolic type, *Numer. Math.*, 102 (2006), 497-522.
- [28] W. Mclean and V. Thomée, Maximum-norm error analysis of a numerical solution via Laplace transformation and quadrature of a fractional order evolution equation, *IMA J. Numer. Anal.*, 30 (2010), 208-230.
- [29] X. C. Wu, W. H. Deng, and E. Barkai, Tempered fractional Feynman-Kac equation: theory and examples, *Phys. Rev. E*, 93 (2016), 032151.
- [30] X. Yang, Numerical contour integral methods for unsteady Stokes equations, *Comput. Math. Appl.*, 75 (2018), 4414-4426.

- [31] Z. Q. Zhou, J. T. Ma, and H. W. Sun, Fast Laplace transform methods for free-boundary problems of fractional diffusion equations, *J. Sci. Comput.*, 74 (2018), 49-69.